의학박사 학위논문

The prognostic implications of tumor infiltrating immune cells and PD-L1 expression in microsatellite-unstable advanced gastric cancers

현미부수체불안정성 진행성위암에서
종양침윤면역세포와 PD-L1의 발현이 갖는
예후적 가치

2017년 8월

서울대학교 대학원
의학과 병리학 전공
김 경 주

현미부수체불안정성 진행성위암에서 종양침윤면역세포와 PD-L1의 발현이 갖는 예후적 가치

지도 교수 강 경 훈

이 논문을 의학박사 학위논문으로 제출함

2017년 7월

서울대학교 대학원

의학과 병리학

김 경 주

김경주의 의학박사 학위논문을 인준함

2017년 6월

위 원 장 _____ (인)

부위원장 _____ (인)

위 원 _____ (인)

위 원 _____ (인)

위 원 _____ (인)

The prognostic implications of tumor infiltrating immune cells and PD-L1 expression in microsatellite-unstable advanced gastric cancers

July 2017

Graduate School of Medicine
Seoul National University

Kyung-Ju Kim

Confirming the Ph.D. Dissertation written by
Kyung-Ju Kim
June 2017

Chair	**_____(Seal)**
Vice Chair	**_____(Seal)**
Examiner	**_____(Seal)**
Examiner	**_____(Seal)**
Examiner	**_____(Seal)**

ABSTRACT

Prognostic implications of tumor infiltrating immune cells and PD-L1 expression in microsatellite-unstable advanced gastric cancers

Kyung-Ju Kim
Department of Medicine, Pathology Major
The Graduate School
Seoul National University

Microsatellite instability-high (MSI-H) gastric cancers are highly immunogenic due to the accumulation of neo-antigens which are produced as a result of frameshift mutation in mismatch-repair-deficient condition. Immunoscore was demonstrated as a powerful prognostic indicator and might be equivalent to the AJCC/UICC-TNM staging system in predicting patients' clinical outcome in malignant tumors. Programmed death ligand-1 (PD-L1) expression was shown to be significantly associated with MSI-H phenotype and high density of tumor

infiltrating lymphocytes (TILs) and tumor associated macrophages (TAMs). In this study, we tried to figure out the efficacy of immunoscore for predicting patients' outcome and how they linked to the TAM and expression status of PD-L1 in tumor cells and immune cells in MSI-high gastric cancers. In 153 patients who were diagnosed as MSI-H advanced gastric cancer, CD3+ TILs, CD8+ TILs and CD68+ TAMs, CD163+ TAMs were analyzed by computerized image analysis system in four different areas (epithelial and stromal compartments of both tumor center and invasive front). The median value of the specific TIL and TAM density was used as the cut-off level to separate the low and high densities of the TILs and TAMs in each area. The immunoscore(I) was quantified by the number of high densities of CD3+ and CD8+ TIL in both regions and compartments (TC and IF within Epithelial and Stromal compartments), ranging from I0 to I8. Each TAM score was determined by adding the number of high densities of CD68+ or CD163+ TAM in both regions and compartments, ranging from score 0 to score 4. Using immunohistochemistry, the expression of PD-L1 was also analyzed in tumor cells (T-PD-L1) and immune cells (I-PD-L1). We found that there was a positive correlation between TILs and TAMs densities in epithelial and stromal compartments. We figure out that high immnoscore was correlated with prolonged overall and disease free survival and high immunoscore in both E and S compartments was an independent good prognostic indicator. Compared with negative expression of T-PD-L1 and I-PD-L1, the positive expression of T-PD-L1 and I-PD-L1 was significantly associated with higher immunoscore and TAM score,

except for the correlation between T-PD-L1 and CD163+ TAM score. A combined survival analysis of PD-L1 expression and immunoscore revealed 4 distinct subgroups with statistically significant difference for overall survival. That is, T-PD-L1 (+)/immunoscore^{Low} group showed the worst, and T-PD-L1 (+)/immunoscore^{High} group showed the best prognosis. There was no significant prognostic difference according to CD68+ TAM score. However, the patients with low density of CD163+ TAM (score 0) was significantly correlated with poor survival outcome compared with those with high density of CD163+ TAM (score 1-4). In conclusion, our study revealed that the immunoscore using CD3+ and CD8+ T lymphocytes subpopulation is a reliable methodology to predict the clinical outcome of MIS-H GC patients and high immunoscore is positively correlated with PD-L1 expression in tumor cells and immune cells in MSI-H GCs. We also demonstrated that PD-L1 expression is mainly induced by adaptive immune resistant mechanism in MSI-H GCs. Furthermore, immunoscore can be a relevant regulator in determining the prognostic role of PD-L1 expression in MSI-H GCs. Although, the prognostic role of TAM was not entirely elucidated, TILs and TAMs are considered to be influenced by each other and the prognostic effect can be determined in proportional balance of both TAMs and TILs in MSI-H GCs.

Keywords: stomach neoplasm; microsatellite instability; tumor infiltrating lymphocytes, tumor associated macrophages, Programmed death ligand-1

Student Number: 2012-31139

CONTENTS

LIST OF TABLES

LIST OF FIGURES

INTRODUCTION

Gastric cancer (GC) is ranked as the fifth most common malignancy in the world and is the third most common cause of death [1]. GC is a heterogeneous disease in terms of molecular carcinogenesis, and microsatellite instability (MSI) accounts for approximately 10% of GCs [2, 3]. MSI refers to genomewide alterations of the number of repeated nucleotides in microsatellites which are located in coding or non-coding regions of genes and results in frameshift mutation. MSI-high (MSI-H) GCs are generally characterized by some distinct clinicopathologic features including better prognosis, preponderance to antral location, intestinal type by Lauren classification, and increased number of tumor infiltrating lymphocytes (TILs), tumor associated macrophages (TAMs) compared with MSI-low (MSI-L) or MS-stable (MSS) GCs [4].

Tumors are heavily infiltrated by many types of inflammatory cells in tumor microenvironment and increasing evidences support that TILs have a prognostic value. Particularly, “Immunoscore” have been demonstrated as a powerful prognostic indicator and might be equivalent to the AJCC/UICC-TNM staging system in predicting patients’ clinical outcome in malignant tumors [5, 6]. The immunoscore is established by the type, density, functional orientation and location of lymphocytes within separate tumor regions (tumor center (TC) and invasive front (IF)) and basically determined by the density of two lymphocyte subpopulations in various combinations, e.g. CD3/CD45RO, CD3/CD8 or CD8/CD45RO [7, 8]. Although most vigorous researches about immunoscore have

been done in colorectal cancers (CRCs), combined immune phenotypes (e.g. CD8/CD3, CD8/CD45RO) with regard to its prognostic value has also been studied in other types of cancers, such as malignant melanomas, breast cancers and prostate cancers [9]. Galon et al. insisted that combination of CD3+ and CD8+ TILs was considered to be clinically feasible because counting of CD3+ and CD8+ TILs was relatively simple and had the excellent reproducibility [10]. High densities of these two markers were demonstrated to be associated with longer disease-free and overall survivals in several cancer types [9]. MSI-H cancers are considered to be highly immunogenic due to the accumulation of neo-antigens that are produced by a frameshift mutation in mismatch-repair-deficient conditions [11]. Therefore, MSI-H GCs are thought to provide an adequate platform for the evaluation of the relevance of tumor infiltrating immune cells in tumor microenvironment.

Programmed death-ligand 1 (PD-L1) is a 40-kDa type 1 transmembrane protein that is involved in the immunoregulatory system during certain conditions such as autoimmune disease, pregnancy, allograft rejection, and cancer [12]. Activation of the programmed cell death-1 (PD-1)/PD-L1 signaling pathway leads to an immunosuppressive tumor microenvironment, which results in immune evasion by tumor cells [13]. Thus, inhibition of the PD-1/PD-L1 signaling axis may be a candidate strategy in cancer immunotherapy. Many clinical trials have revealed that anti-PD-1/PD-L1 therapy is effective against various types of tumors, including malignant melanoma, non-small cell lung cancer, and renal cell carcinoma [14,15]. A phase Ib clinical trial showed that pembrolizumab, an anti-

PD-1 antibody, displays promising antitumor activity against GC and has manageable toxicities [16]. However, a limited number of patients was enrolled (n = 39) and only 22% of patients with a partial response have been reported in this trial thus far [16]. A recent phase II trial reported that mismatch-repair status predicts a survival benefit during blockade of the immune checkpoint system in colorectal cancer (CRC) patients [17]. In this regard, several studies of CRC and GC demonstrated that PD-L1 expression in tumor cells and infiltrating immune cells is significantly associated with the MSI-H phenotype and a high density of tumor-associated immune cells [18-21].

Monocytes are considered to have functional and phenotypic plasticity that enables them to differentiate into two polarization states - M1 and M2 macrophages - depending on the cytokine milieu in the tumor microenvironment [22]. Classically activated (M1) macrophages are induced by T helper type 1-like cytokines such as interferon-γ and are involved in anti-microbial and tumoricidal activity. In contrast, alternatively activated (M2) macrophages are induced by T helper type 2 cytokines including interleukin-4 (IL-4), IL-10 and IL-13 and show immunoregulatory, anti-inflammatory and tumor-promoting activity. In general, TAMs are considered to resemble the M2 phenotype more than the M1 phenotype [23]. Therefore, TAMs are thought to be associated with poor survival of cancer patients by promoting invasion, metastasis, angiogenesis and lymphangiogenesis. In fact, TAMs have been related to decreased survival in many solid tumors (e.g., ovary [24], melanoma [25], lung [26,27], endometrium [28], breast [29,30] and kidney [31,32])

but not all (e.g., GCs, colorectal cancers (CRCs)). Several studies in GCs and CRCs have demonstrated better prognosis in patients with a high density of TAMs [33-36], which indicates that the functional role of TAMs could be different depending on type of tissue and cancer.

In the current study, we evaluated whether the immunoscore methodology is applicable to predict the risk of recurrence and death in MSI-H GCs patients. Secondly, we analyzed PD-L1 expression in context of tumor microenvironment and assess 1) how they were linked to the immunoscore and tumor associated immune cells and 2) the differential prognostic value of PD-L1 expression according to the density of TILs. And we also evaluate the prognostic significance of CD68+ and CD163+ TAMs MSI-H GCs.

MATERIALS AND METHODS

Patients and specimens

A total 153 GC formalin-fixed paraffin-embedded tissue were collected from the pathology archives of Seoul National University Hospital, Seoul, Korea. All tumor samples were derived from the patients who received surgical resection with extended lymph node dissection at our institutions between 2004 and 2009. In our institution, MSI status was routinely evaluated in resected GC specimens by the molecular pathology laboratory. Among 1,706 patients, 153 (8.7%) of advanced GC with MSI-H were identified. Clinicopathological information, including age, sex, tumor site, tumor differentiation, tumor depth, lymph node metastasis, presence of lymphatic, vascular and perineural invasion, TNM stage, Lauren classification, Ming classification, date of surgery, date of last follow-up and date of recurrence or death, were collected retrospectively from the electronic medical records. We evaluated overall survival (OS) and disease free survival (DFS). OS was assessed from the date of GC surgery to the date of death or the last clinical follow-up before December 31, 2015 and DFS was defined as the duration from the date of surgery to death, tumor recurrence or date of the last follow-up before December 31, 2015. The average OS time was 2552 days and ranged from 35 to 4241 days. The average DFS time was 1721 days and ranged from 10 to 4019 days. In this study, death and recurrence occurred in 46 (30.1%) and 44 (28.7%) cases out of all patients with MSI-H advanced GCs, respectively. Histologic grading and tumor staging were based on the American Joint Committee on Cancer (AJCC)

Staging Manual Seventh Edition. This study was approved by the institutional review board of Seoul National University Hospital.

DNA extraction and determination of MSI

The methods used for the MSI analysis have been previously described [37]. Briefly, manually microdissected tumor samples were collected into 1.5 mL microtubes containing 50 -μL lysis buffer (100 mM Tris-HCl, 0.5% Tween-20, 1 mM EDTA and 20 μg/ml proteinase K) and incubated for 24 to 48 hour at 55°C until the tissue-containing lysis buffer became cleared. The proteinase K was inactivated by incubation at 95°C for 10 min. Extracted genomic DNA was stored at -20°C until use. MSI status was assessed at the following loci according to the National Institutes of Health guidelines: BAT25, BAT26, D2S123, D5S346 and D17S250. We defined tumors as MSI-H when two or more markers showed instability, MSI-L when one marker showed instability, and MSS when none of the markers were unstable.

GC tissue Microarray and Immunohistochemistry

Tissue microarrays (TMAs) were constructed as previously described [37]. Tissue cores (2 mm in diameter) containing 2 representative tumor regions –TC and IF – were punched from individual donor tissue blocks and transferred to new recipient blocks using a trephine apparatus. One tissue core from TC region and two cores

from IF regions were obtained from each case, and 9 TMA blocks from 153 cases were constructed (Figure 1).

Using 4-μm thick TMA tissue sections, immunohistochemical staining for each marker was conducted using antibodies against CD3 (Pan-T lymphocyte marker) (rabbit polyclonal, 1:100; DAKO, Glostrup, Denmark); CD8 (cytotoxic T cell marker) (SP16, 1:100; Neomarkers, Fremont, CA); CD68 (overall infiltrated TAM marker) (EBM11, 1:100; Dako, Glostrup, Denmark); CD163 (M2 macrophage marker) (10D6, 1:100; Novocastra Lab, Newcastle, UK); hMLH1 (CMC869, 1:50; Rocklin, CA, USA); hMSH2 (FE11, 1:200; Invitrogen, Camarillo, CA, USA) and PD-L1 (E1L3N, 1:50; Cell Signaling Technology, Danvers, MA, USA).

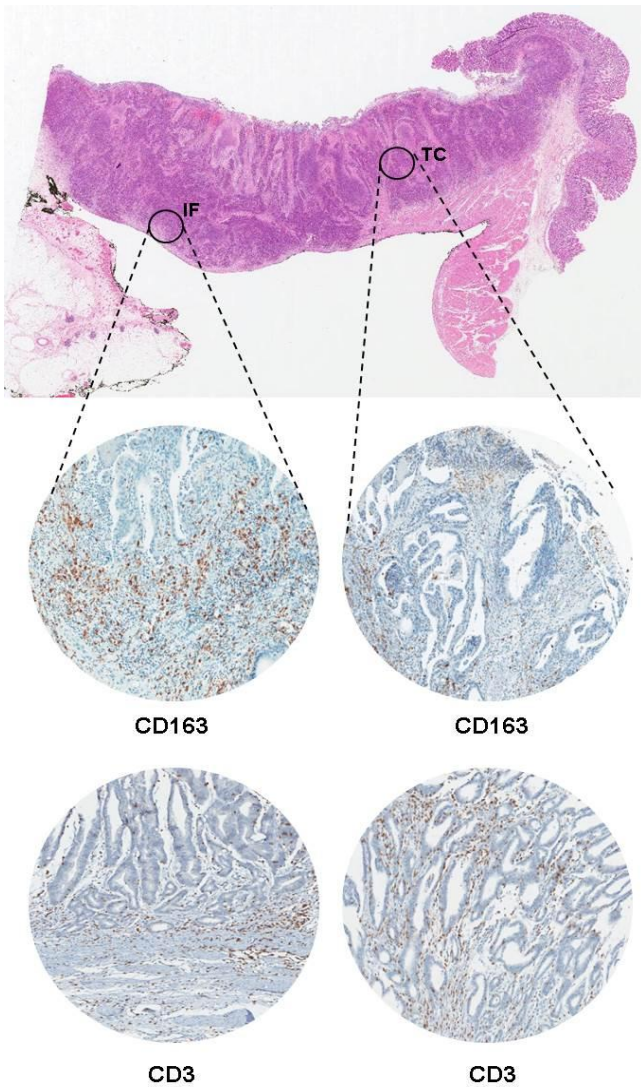

Figure 1. Representative image of the IF and TC in MSI-H advanced GCs. H&E section of GCs (original magnification, 12.5x) (top) showing each regions of the tumor: IF and TC. Immunohistochemical staining for CD3 and CD163 in each region (bottom).

Abbreviations: H&E, Hematoxylin and Eosin, IF, invasive front; TC, tumor center

Determination of immunoscore

All immunostained TMA slides were scanned under high-power magnification (200x) using a scanner system (ScanScope XT; Aperio Technology, Vista, CA, USA). The Nuclear V9 algorithm of Image-Scope software (Aperio Techonology) was used to evaluate the densities of CD3+ or CD8+ lymphocytes as numbers of CD3+ or CD8+ lymphocytes divided by a total area of selected foci (cells per square millimeter) (Figure 2). The density of CD3+ or CD8+ TIL was analyzed in the epithelial (E) and stromal (S) compartments in the same core, separately, which generated densities in four different areas (E and S compartments of TC and IF regions (E-TC, S-TC, E-IF, and S-IF areas). The median value of the specific TIL density was used as the cut-off level to separate the low and high densities of the TILs in each area. The immunoscore (I) of E and S compartments was separately assessed and designated as E-I and S-I, respectively. The E-I and S-I were quantified by the number of high densities of CD3+ or CD8+ TILs in both regions and compartments (E and S compartments of the TC and IF regions). With combined analysis of two or four areas, tumor was given a sum score ranging from 0 to 2 for two areas (E-CD3-I, E-TC + E-IF for CD3+ TILs; S-CD3-I, S-TC + S-IF for CD3+ TILs; E-CD8-I, E-TC + E-IF for CD8+ TILs; S-CD8-I, S-TC + S-IF for CD8+ TILs) and ranging from 0 to 4 for four areas (E-CD3/CD8-I, E-TC + E-IF for CD3+ and CD8+ TILs; S-CD3/CD8-I, S-TC + S-IF for CD3+ and CD8+ TILs). And then total immunoscore (T-CD3/CD8-I) was determined by combining E-CD3/CD8-I and S-CD3/CD8-I which ranged from T-CD3/CD8-I0 to T-CD3/CD8-

I8. For example, T-CD3/CD8-I8 refers to a case with high densities of CD3+ and CD8+ cells in the TC and IF regions within the S and E compartments, whereas T-CD3/CD8-I0 refers to a case with low densities of CD3+ and CD8+ cells in four different tumor areas. Figure 3 shows how this scoring system was applied in this study.

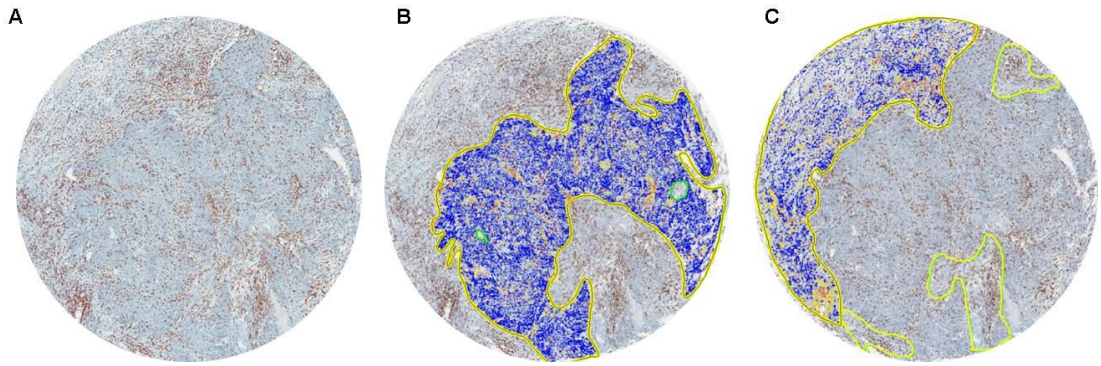

Figure 2. Representative image of the counting the CD8+ TILs density. A. By means of automatic image analysis system (ScanScope XT; Aperio), tumor density of positively stained cells was measured in **B.** epithelial compartment and **C.** stromal compartment.

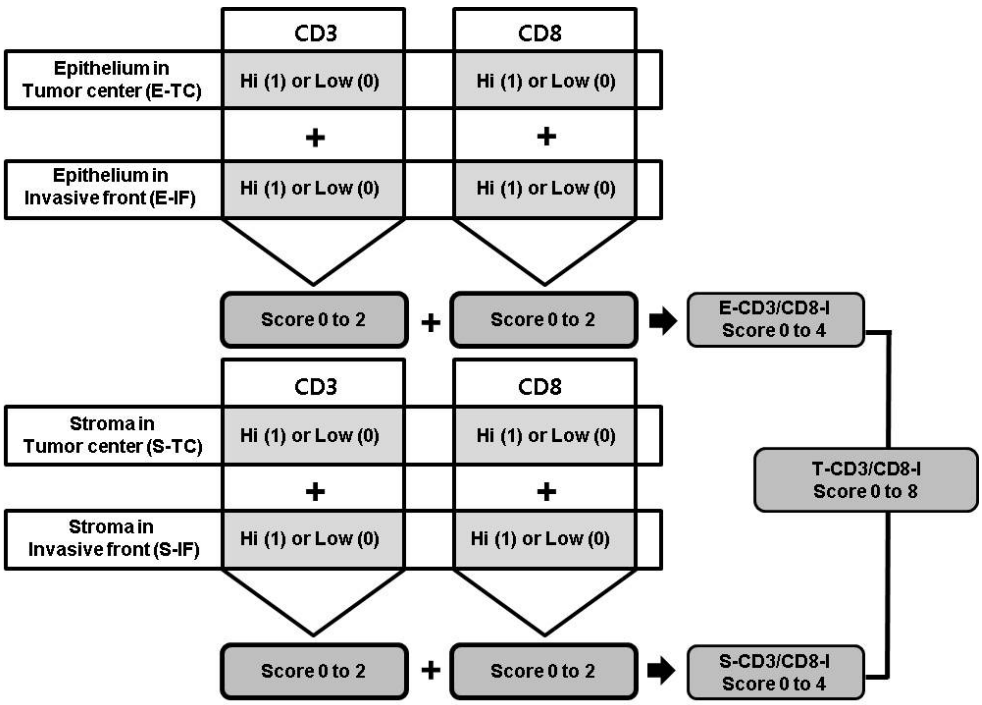

Figure 3. Development of the immunoscore system. The immunoscore (I) of E and S compartments was separately assessed and designated as E-I and S-I, respectively. The E-I and S-I were quantified by the number of high densities of CD3+ or CD8+ TILs in both regions and compartments (E and S compartments of the TC and IF regions). With combined analysis of two or four areas, tumor was given a sum score ranging from 0 to 2 for two areas (E-CD3-I; S-CD3-I; E-CD8-I; S-CD8-I) and ranging from 0 to 4 for four areas (E-CD3/CD8-I; S-CD3/CD8-I). And then total immunoscore (T-CD3/CD8-I) was determined by combining E-CD3/CD8-I and S-CD3/CD8-I which ranged from T-CD3/CD8-I0 to T-CD3/CD8-I8.

Abbreviations: I, immunoscore; E, epithelial compartment; S, stromal compartment; T, total compartment; TC, tumor center; IF, invasive front

Evaluation of PD-L1 expression

PD-L1 expression was assessed separately in tumor cells (T-PD-L1) and stromal immune cells (I-PD-L1). The intensity of membranous-to-cytoplasmic staining in tumor cells and infiltrating immune cells in the stroma was initially scored on a scale of 0 to 3, as follows: negative (0), weak (1+), moderate (2+), and strong (3+). PD-L1 expression was determined to be positive when moderate (2+) and strong (3+) intensities were observed in at least 5% of the tumor cells (T-PD-L1 (+)) in at least 5% of the immune cells (I-PD-L1 (+)). A higher score was given if three cores from the same tumor exhibited different PD-L1 expression scores. Representative images of the tumors that demonstrated T-PD-L1 (+)/I-PD-L1 (-) and T-PD-L1 (-)/I-PD-L1 (+) with matched hematoxylin and eosin-stained samples are shown in Figure 4.

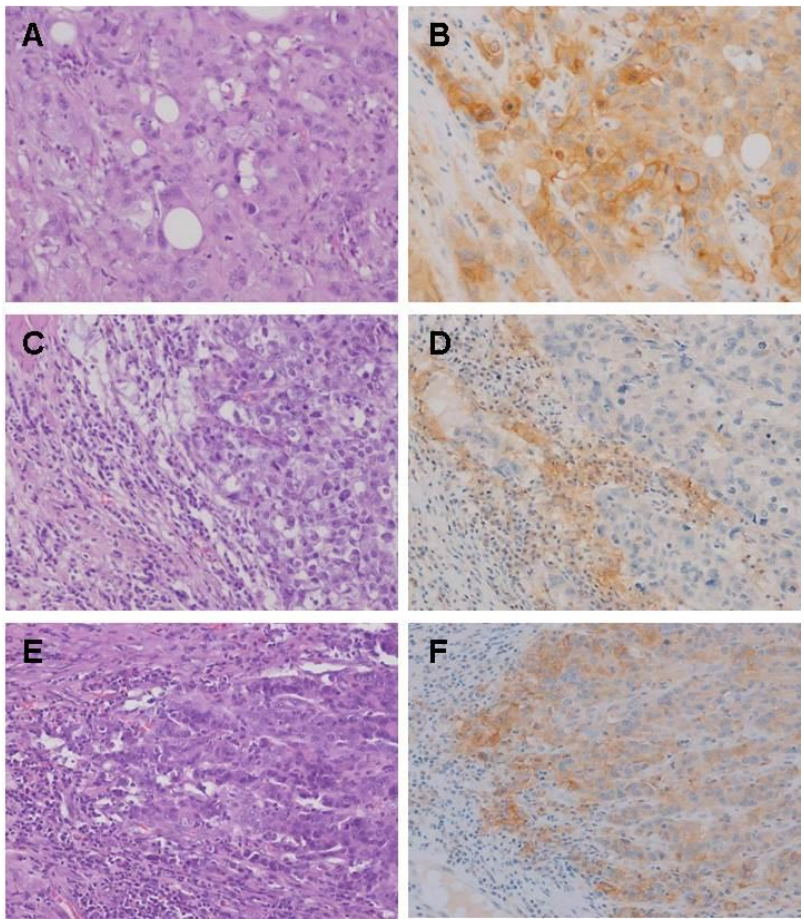

Figure 4. Immunohistochemical staining results of the PD-L1 and its matched H&E staining samples. A and B. Representative images of T-PD-L1 (+)/I-PD-L1 (-) (A: H&E, x200) and its histological features (B: IHC, x200). **C and D.** Representative images of T-PD-L1 (-)/I-PD-L1 (+) (C: H&E, x200) and its histological features (D: IHC, x200). **E and F.** Representative images of T-PD-L1 (+)/I-PD-L1 (+) (E: H&E, x200) and its histological features (F: IHC, x200).

Abbriviations: H&E, Hematoxylin and Eosin; T-PD-L1, PD-L1 expression in tumor cells; I-PD-L1, PD-L1 expression in stromal immune cells; IHC, immunohistochemical staining

Determination of TAM score

All immunostained TMA slides were scanned under high-power magnification (200x) using a scanner system (ScanScope XT; Aperio Technology, Vista, CA, USA). Because CD68 and CD163 immunohistochemical staining was detected on the cell membrane and cytoplasm, which have a rough contour with variable morphology, the determination of the density by automatic counting of the number of infiltrated macrophages in selected areas using a computerized system was impossible. Instead, we used the positive pixel count v9 algorithm of ImageScope software (Aperio Technology), which defined macrophage density as areas of positively stained cells divided by all selected areas (Figure 5). To validate the accuracy of this method, we manually counted the number of the infiltrated macrophages in defined areas of 20 random cases including 10 CD68- and 10 CD163-stained cases. The correlation between the manual count and the positive pixel count of macrophages in the same area of the core was evaluated using Spearman's rho analysis. A strong positive correlation between the two values was found (Spearman's rank correlation coefficient r = 0.821, $p < 0.001$). In this way, the positive pixel count could be used as an alternative method for the enumeration of infiltrated CD68+ and CD163+ TAMs. For each tissue sample with TAMs, GC was scored 0 or 1 when the measured density of TAMs was below or above the median value of the respective TAM density in the specific area. With combined analysis of two or four areas, a tumor was given a sum score ranging from 0 to 2 for two areas or from 0 to 4 for four areas. Figure 5 shows how this scoring system

was applied in this study. For example, in cases with CD68+ TAMs, score 4 refers to a tumor with a high density of CD68+ cells in four different areas (S-IF, E-IF, S-TC, and E-TC) at the same time.

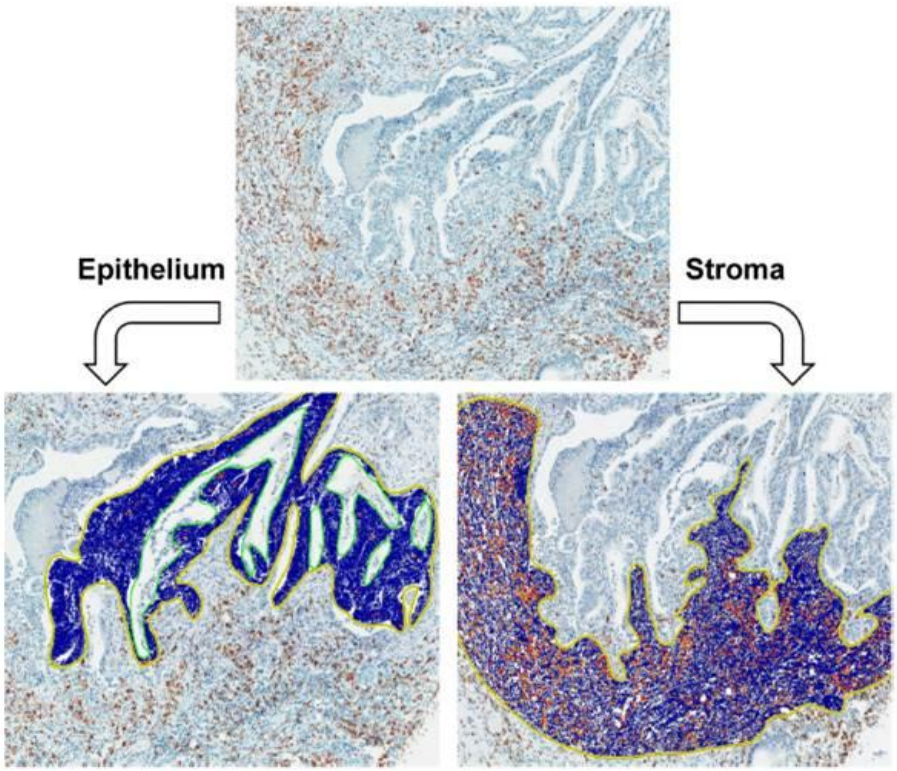

Figure 5. Immunohistochemical staining of the CD68 and CD163 and measurement of the density of the CD68+ and CD163+ TAMs. Using the automatic image analysis system (ScanScope XT; Aperio) for positive pixel count v9 algorithm, the density of CD68+ or CD163+ TAM was measured separately in the epithelium (left lower) and stroma (right lower).

Statistical analysis

The correlation of TILs and TAMs was analyzed using Spearman's rank correlation test. The categorical variables were compared using Pearson's chi-square test or Fisher's exact test (for cases with an n value <10). Differences in mean value were analyzed using 2-tailed Student's *t*-test. Kaplan-Meier survival analysis was performed to compare OS and DFS between two subgroups. Multivariate survival Cox proportional hazards regression model was used to adjust variables that may have been statistically significant for prognosis in univariate analysis. Statistical analysis was performed using the SPSS (Statistical Package for the Social Sciences) software program (version 20.0; Chicago, IL, USA). All p values were two sided, and $p<0.05$ was considered statistically significant.

RESULTS

Quantification analysis of TILs in MSI-H GCs

Median and mean values of each TIL/TAM density are listed in Table 1 and Table 2. The correlations of the densities TILs and TAMs in epithelial and stromal compartments (E-CD68+ TAM, S-CD68+ TAM, E-CD163+ TAM, S-CD163+ TAM, E-CD3+ TIL, S-CD3+ TIL, E-CD8+ TIL and S-CD8+ TIL) are summarized in Table 3. With regard to TILs, positive correlations were observed regardless of their location. Positive correlations were also shown between TAMs regardless of their compartments. However, between different types of macrophages, the density of S-CD3+ TIL did not correlate with the densities of E-CD68+ TAM, S-CD68+ TAM, E-CD163+ TAM, S-CD163+ TAM. In addition, E-CD3+ TIL and S-CD68+ TAM were not correlated.

Comparison of the values of CD68+ and CD163+ TAMs between the E compartment and S compartment revealed a significantly higher amount of TAMs in S compartment than in E compartment (Student *t*-test, $p < 0.001$ for CD68+ and CD163+ TAMs in E-TC vs. S-TC; $p < 0.001$ for CD68+ and CD163+ TAMs in E-IF vs. S-IF) (Figure 6). For CD3+ and CD8+ TILs, a similar trend for a higher infiltration of TILs in S compartment compared with E compartment was observed (Student *t*-test, $p < 0.001$ for CD3+ TILs in E-TC vs. S-TC and in E-IF vs. S-IF; $p = 0.002$ for CD8+ TILs in E-TC vs. S-TC; $p < 0.001$ for CD8+ TILs in E-IF vs. S-IF) (Figure 6).

Table 1. Median and mean values of the density of the CD3+ and CD8+ TIL in four different tumor areas.

	Median (cells/mm^2)	Mean (cells/mm^2)	Range (cells/mm^2)
E-TC CD3+ TIL	261	362	0 - 1343
S-TC CD3+ TIL	592	698	7 - 2310
E-IF CD3+ TIL	385	307	0 - 1350
S-IF CD3+ TIL	760	864	0 - 3162
E-TC CD8+ TIL	229	305	0 - 1705
S-TC CD8+ TIL	384	405	0 - 1373
E-IF CD8+ TIL	315	387	0 - 1518
S-IF CD8+ TIL	462	569	0 - 2232

Abbreviations: E, epithelial compartment; TC, tumor center; S, Stromal compartment; IF, invasive front

Table 2. Median and mean values of the density of the CD68+ and CD163+ TAM in four different tumor areas.

	Median	Mean	Range
E-TC CD68+ TAM	0.067	0.072	0.00 – 0.24
S-TC CD68+ TAM	0.139	0.156	0.01 – 0.44
E-IF CD68+ TAM	0.067	0.080	0.01 – 0.64
S-IF CD68+ TAM	0.151	0.174	0.01 – 0.52
E-TC CD163+ TAM	0.030	0.044	0.00 – 0.20
S-TC CD163+ TAM	0.096	0.132	0.01 – 0.41
E-IF CD163+ TAM	0.048	0.059	0.01 – 0.20
S-IF CD163+ TAM	0.130	0.145	0.01 – 0.46

Abbreviations: E, epithelial compartment; TC, tumor center; S, Stromal compartment; IF, invasive front

Table 3. Correlation of the TIL and TAM density according to each region in MSI-H GCs.

		E-CD68+ TAM	S-CD68+ TAM	E-CD163+ TAM	S-CD163+ TAM	E-CD3+ TIL	S-CD3+ TIL	E-CD8+ TIL	S-CD8+ TIL
E-CD68+ TAM	r	1	0.303	0.699	0.206	0.363	-0.127	0.288	0.416
	p-value	(-)	0.001	<0.001	0.021	<0.001	0.187	0.002	<0.001
S-CD68+ TAM	r		1	0.270	0.630	0.166	0.075	0.334	0.312
	p-value		(-)	0.002	<0.001	0.087	0.437	<0.001	0.001
E-CD163+ TAM	r			1	0.535	0.449	-0.084	0.273	0.503
	p-value			(-)	<0.001	<0.0010	0.386	0.003	<0.001
S-CD163+ TAM	r				1	0.338	-0.02	0.215	0.342
	p-value				(-)	<0.001	0.835	0.022	<0.001
E-CD3+ TIL	r					1	0.465	0.583	0.665
	p-value					(-)	<0.001	<0.001	<0.001
S-CD3+ TIL	r						1	0.443	0.355
	p-value						(-)	<0.001	<0.001
E-CD8+ TIL	r							1	0.792
	p-value							(-)	<0.001
S-CD8+ TIL	r								1
	p-value								(-)

Abbreviations: r, correlation coefficient; E, epithelial compartment; S, Stromal compartment

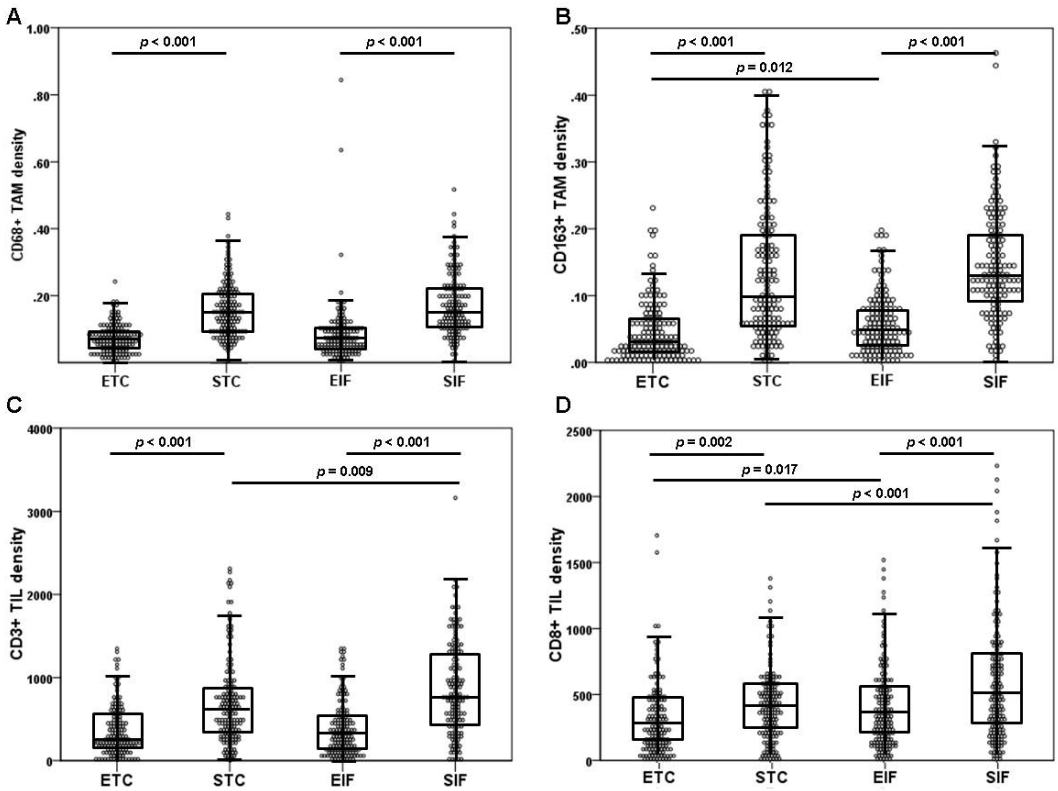

Figure 6. Box plots comparing the density of the CD68+ TAMs, CD163+ TAMs, CD3+ TILs and CD8+ TILs according to different tumor areas (E-TC, S-TC, E-IF and S-IF) A. The density of CD68+ TAMs is significantly higher in S compartment rather than in E compartment. **B.** The density of CD163+ TAMs is shown to be higher in S compartment than in E compartment. In addition, CD163+ TAM density in E-IF is significantly higher in E-TC. **C.** The density of CD3+ TILs is shown to be higher in S compartment than in E compartment. Moreover, CD3+ TIL density in S-IF is significantly higher than in S-TC. **D.** The density of CD8+ TILs is illustrated to be higher in S compartment than in E compartment. In

addition, CD8+ TIL density in E-IF and S-IF is significantly higher in E-TC and S-TC, respectively. Statistical significance was evaluated using a Student *t*-test.

Abbreviations : E-TC, epithelial compartment in tumor center; S-TC, stromal compartment in tumor center; E-IF, epithelial compartment in invasive front; S-IF, stromal compartment in invasive front

The prognostic implications of immunoscore in MSI-H GCs

With univariate survival analysis of CD3-I and CD8-I in each compartments, patients with a low immunoscore showed significantly lower DFS compared with patients with a high immunoscore (score 0 vs. score 2: hazard ratio (HR), 0.301 for E-CD3-I; HR, 0.311 for S-CD3-I; HR, 0.422 for E-CD8-I; HR, 0.279 for S-CD8-I, all $p < 0.03$) (Table 4). Similar results for OS were observed in E-CD3-I and S-CD8-I (score 0 vs. score 2: HR, 0.402 for E-CD3-I; HR, 0.229 for S-CD8-I, all $p < 0.03$) (Table 4). However, marginal significance was observed between the two groups (score 0 vs. score 2) in case of E-CD8-I and S-CD3-I (score 0 vs. score 2: HR, 0.555; $p = 0.112$ for E-CD8-I and HR, 0.517; $p = 0.105$ for S-CD3-I) (Table 4). In Kaplan-Meier analysis, repartitions of the cases according to the CD3/CD8-I had a borderline significance to discriminate the clinical outcome for OS among 5 subgroups (CD3/CD8-I0 vs. CD3/CD8-I1 vs. CD3/CD8-I2 vs. CD3/CD8-I3 vs. CD3/CD8-I4) in both compartments (E and S compartment) ($p = 0.060$ for both of E-CD3/CD8-I and S-CD3/CD8-I), but higher scores could not guarantee a better prognosis among patients with CD3/CD8-I1, CD3/CD8-I2 and CD3/CD8-I3 (Figure 7A & Figure 8A). With regard to DFS, higher immunoscore appeared to decrease the risk of relapse in both compartments but statistical significance was not reached ($p = 0.081$ for E-CD3/CD8-I and 0.079 for S-CD3/CD8-I, respectively) (Figure 7D & Figure 8D). However, CD3/CD8-I0 and CD3/CD8-I4 subgroup showed a statistically significant survival difference in both compartment ($p = 0.016$ for E-CD3/CD8-I and $p = 0.004$ for S-CD3/CD8-I). When the cohorts were

reclassified into three subgroups (CD3/CD8-I0 and CD3/CD8-I1 vs. CD3/CD8-I2 and CD3/CD8-I3 vs. CD3/CD8-I4), the patients with CD3/CD8-I4 showed the best and the patients with CD3/CD8-I0 or CD3/CD8-I1 showed the worst DFS (p = 0.03 for both of E-CD3/CD8-I and S-CD3/CD8-I) (Figure 7E & figure 8E). When we lumped the patients together into two subgroup (CD3/CD8-I0 to CD3/CD8-I3 vs. CD3/CD8-I4), the CD3/CD8-I4 group had a significant survival advantage for OS (p = 0.007 for E-CD3/CD8-I and p = 0.019 for S-CD3/CD8-I) (Figure 7C & Figure 8C) and DFS (p = 0.016 for E-CD3/CD8-I and p = 0.019 for S-CD3/CD8-I) compared with the remainders in both compartment (Figure 7F & Figure 8F). The total immunoscore (T-CD3/CD8-I) was determined by sum score of E-CD3/CD8-I and S-CD3/CD8-I, ranging to score 0 to score 8. Although the increased risk of relapse or death was not followed the T-CD3/CD8-I (p = 0.141 for OS; p = 0.036 for DFS) (Figure 9A & Figure 9C), tumors could be largely divided into two subgroups (Low (T-CD3/CD-I0 to T-CD3/CD-I4) vs. High (T-CD3/CD-I5 to T-CD3/CD-I8)) (p = 0.005 for OS; p = 0.002 for DFS) (Figure 9B & Figure 9D). The associations between the clinicopathological parameters of MSI-H GCs and the Immunoscore are summarized in Table 5. Briefly, E-I4 subgroup was closely associated with less frequency of lymphatic invasion (p < 0.001), perineural invasion (p = 0.004), lymph node (LN) metastasis (p = 0.015), and lower AJCC tumor stage (p = 0.012). S-CD3/CD8-I4 subgroup had less frequent lymphatic invasion compared to the remainders (p = 0.002).

Table 4. Univariate analysis of OS and DFS among patients with MSI-H GCs.

Variables	*n*	Overall survival		*n*	Disease free survival[b]	
		HR (95% CI)	*p*-value		HR (95% CI)	*p*-value
Age			0.042			0.250
≤50	16	1		12	1	
>50	137	2.209 (1.029-4.743)		129	1.745 (0.675-4.508)	
Tumor differentiation			0.126			0.933
WD/MD	67	1		63	1	
PD/Other	86	1.605 (0.875-2.945)		78	1.03 (0.520-2.040)	
Ming			0.004			0.024
Expanding	40	1		39	1	
Infiltrative	113	4.44 (1.589-12.408)		102	3.316 (1.168-9.419)	
Lymphatic invasion			0.004			0.033
Absent	54	1		54	1	
Present	99	3.084 (1.438-6.616)		87	2.37 (1.073-5.237)	
Vascular invasion			0.019			0.023
Absent	129	1		121	1	
Present	24	2.253 (1.143-4.441)		20	2.516 (1.137-5.567)	
Perineural invasion			0.001			0.028
Absent	97	1		93	1	
Present	56	2.754 (1.530-4.922)		48	2.125 (1.084-4.163)	
AJCC stage			<0.001			<0.001
I/II	92	1		92	1	
III/IV	61	7.975 (3.946-16.118)		49	5.283 (2.257-10.857)	
pT stage			<0.001			0.004
pT 2/pT3	121	1		118	1	
pT4	32	3.639 (2.013-6.577)		23	2.900 (1.413-5.953)	
pN stage			<0.001			<0.001
pN0-N2	119	1		116	1	
pN3	34	5.101 ((2.847-9.139)		25	3.680(1.817-7.455)	
E-CD3-I[a]			0.063			0.040
Score 2	53	1		50	1	
Score 1	40	2.4 (1.050-5.486)	0.038	36	2.701 (0.981-7.436)	0.055
Score 0	50	2.424 (1.096-5.361)	0.029	47	3.32 (1.309-8.421)	0.012
E-CD8-I[a]			0.183			0.075
Score 2	61	1		58	1	
Score 1	23	1.763 (0.881-3.527)	0.109	20	1.302 (0.408-4.115)	0.655

Score 0	59	1.993 (0.852-4.663)	0.112	55	2.369 (1.100-5.102)	0.028
S-CD3-I[a]			0.244			0.048
Score 2	49	1		45	1	
Score 1	43	1.747 (0.775-3.935)	0.178	39	2.149 (0.781-5.913)	0.139
Score 0	51	1.887 (0.876-4.068)	0.105	49	3.211 (1.265-8.149)	0.014
S-CD8-I[a]			0.014			0.042
Score 2	45	1		43	1	
Score 1	50	3.696 (1.372-9.958)	0.010	46	3.115 (1.110-8.746)	0.031
Score 0	48	4.252 (1.594-11.340)	0.004	44	3.578 (1.299-9.857)	0.014
E-CD3/CD8-I[a]			0.035			0.043
Score 4	44	1		43	1	
Score 2,3	35	3.338 (1.299-8.806)	0.013	30	2.251 (0.714-7.099)	0.166
Score 0,1	64	2.905 (1.182-7.141)	0.02	60	3.423 (1.290-9.083)	0.013
E-CD3/CD8-I[a]			0.011			0.023
Score 4	44	1		43	1	0.023
Score 0-3	99	3.07 (1.295-7.276)		90	3.03 (1.169-7.851)	
S-CD3/CD8-I[a]			0.080			0.047
Score 4	33	1		31	1	
Score 2,3	49	3.006 (1.005-8.993)	0.049	44	2.948 (0.822-10.569)	0.097
Score 0,1	61	3.361 (1.161-9.733)	0.025	58	4.469 (1.321-15.122)	0.016
S-CD3/CD8-I[a]			0.027			0.029
Score 4	33	1		31	1	
Score 0-3	110	3.204 (1.144-8.974)		102	3.754 (1.145-12.310)	
T-CD3/CD8-I[a]			0.007			0.003
High	63	1		59	1	
Low	80	2.573 (1.296-5.109)		74	3.522 (1.528-8.120)	
CD68+ TAM score[a]			0.199			0.127
Score 4	22	1		22	1	
Score 1-3	82	0.566 (0.231-1.388)	0.214	82	0.602 (0.245-1.476)	0.267
Score 0	20	1.193 (0.418-3.402)	0.742	20	1.427 (0.245-1.476)	0.493
CD163+ TAM score[a]			0.035			0.063
Score 4	21	1		21	1	
Score 1-3	82	0.561 (0.215-1.464)	0.238	81	0.527 (0.213-1.306)	0.166
Score 0	21	1.688 (0.599-4.757)	0.322	21	1.392 (0.518-3.744)	0.512
CD68+ TAM score[a]			0.170			0.078
Score 1-4	104	1			1	
Score 0	20	1.816 (0.775-4.254)			2.071 (0.922-4.652)	
CD163+ TAM score[a]			0.017			0.045
Score 1-4	103	1			1	

Score 0	21	2.613 (1.187-5.748)	2.226 (1.018-4.867)

[a]Included only for patients with available TMA data.

[b]The patients diagnosed as Stage IV were excluded in survival analysis for DFS.

Abbreviations: HR, Hazard ratio; W/D, well differentiated; M/D, moderately differentiated; P/D, poorly differentiated; AJCC, American Joint Committee on Cancer; E, epithelial compartment; S, stromal compartment; T, total compartment; I, immunoscore

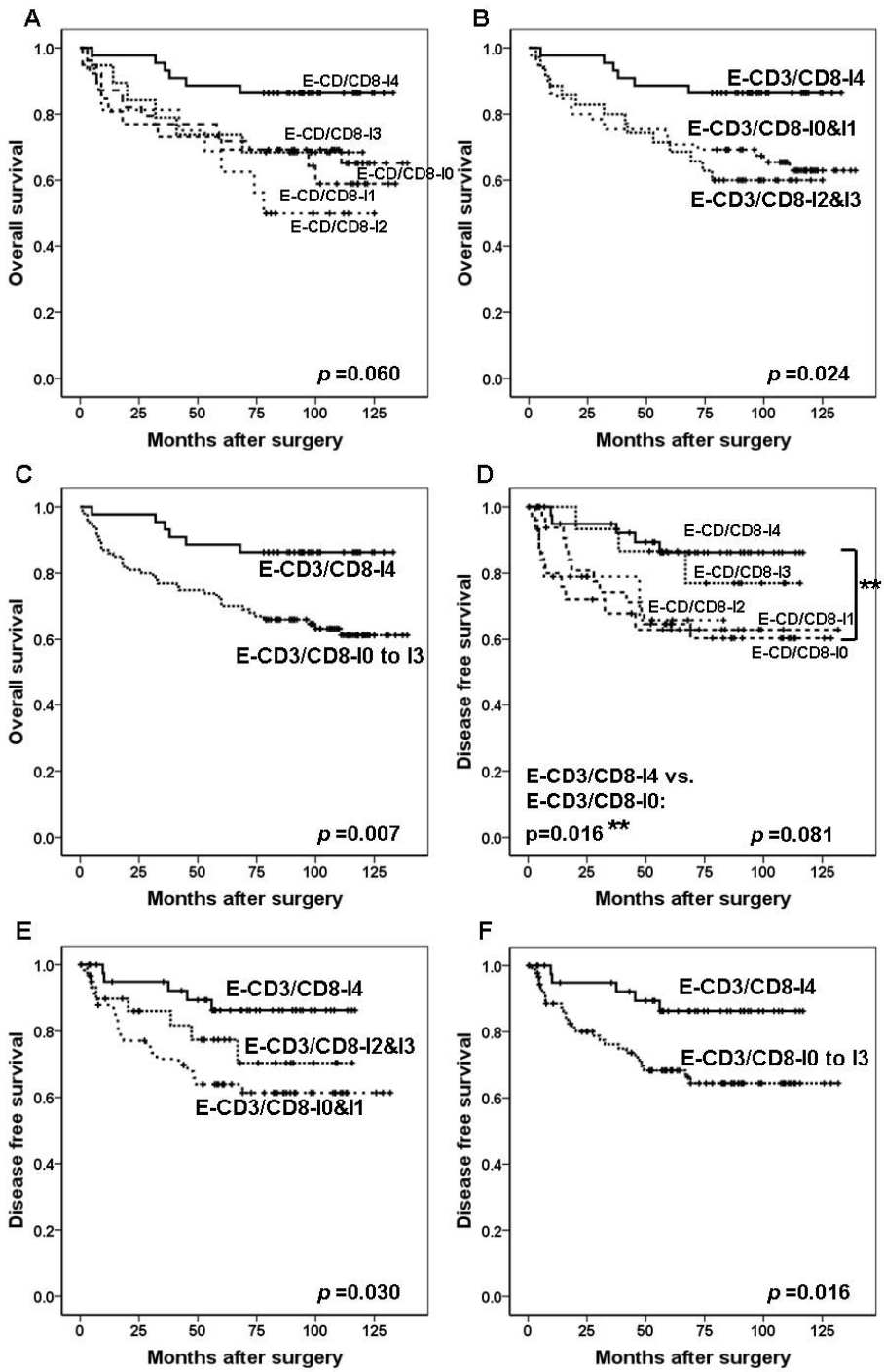
A
Overall survival
E-CD/CD8-I4
E-CD/CD8-I3
E-CD/CD8-I0
E-CD/CD8-I1
E-CD/CD8-I2
p =0.060
Months after surgery
B
Overall survival
E-CD3/CD8-I4
E-CD3/CD8-I0&I1
E-CD3/CD8-I2&I3
p =0.024
Months after surgery
C
Overall survival
E-CD3/CD8-I4
E-CD3/CD8-I0 to I3
p =0.007
Months after surgery
D
Disease free survival
E-CD/CD8-I4
E-CD/CD8-I3
E-CD/CD8-I2
E-CD/CD8-I1
E-CD/CD8-I0
**
E-CD3/CD8-I4 vs.
E-CD3/CD8-I0:
p=0.016 **
p =0.081
Months after surgery
E
Disease free survival
E-CD3/CD8-I4
E-CD3/CD8-I2&I3
E-CD3/CD8-I0&I1
p =0.030
Months after surgery
F
Disease free survival
E-CD3/CD8-I4
E-CD3/CD8-I0 to I3
p =0.016
Months after surgery

Figure 7. Kaplan-Meier survival analysis with log-rank test of the E-CD3/CD8-I. A. Survival curves for the time of OS according to the E-CD3/CD8-I (No. of patients; E-CD3/CD8-I0, 38; E-CD3/CD8-I1, 26; E-CD3/CD8-I2, 16; E-CD3/CD8-I3, 19; E-CD3/CD8-I4, 44). **B.** Survival curves for OS of E-CD3/CD8-I0 and E-CD3/CD8-I1 (*n* = 64) vs. E-CD3/CD8-I2 and E-CD3/CD8-I3 (*n* = 35) vs. E-CD3/CD8-I4 (*n* = 44). **C.** Survival curves for OS of E-CD3/CD8-I0 to E-CD3/CD8-I3 (*n* = 99) vs. E-CD3/CD8-I4 (*n* = 44). **D.** Survival curves for the time of DFS according to the E-CD3/CD8-I (No. of patients; E-CD3/CD8-I0, 35; E-CD3/CD8-I1, 25; E-CD3/CD8-I2, 15; E-CD3/CD8-I3, 15; E-CD3/CD8-I4, 43). The patients who diagnosed as TNM stage IV were excluded in survival analysis for DFS. **Significant difference was observed for DFS duration between patients with score 4 and score 0. **E.** Survival curves for DFS of E-CD3/CD8-I0 and E-CD3/CD8-I1 (*n* = 60) vs. E-CD3/CD8-I2 and E-CD3/CD8-I3 (*n* = 30) vs. E-I4 (*n* = 43). **F.** Survival curves for DFS of E-CD3/CD8-I0 to E-CD3/CD8-I3 (*n* = 90) vs. E-CD3/CD8-I4 (*n* = 43).

Abbreviations: E, epithelial compartment, I, immunoscore, OS, overall survival; DFS, disease free survival

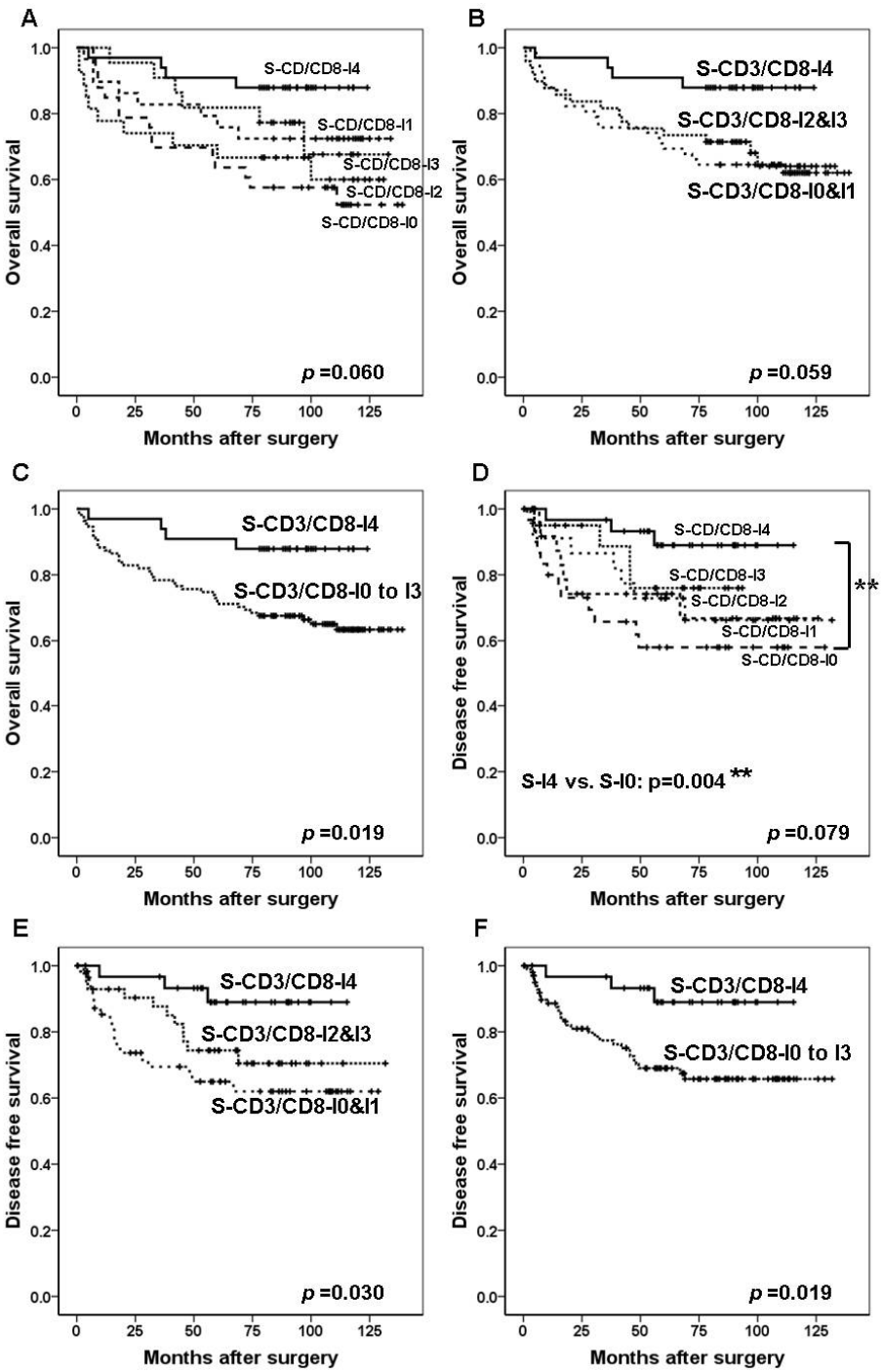
A
Overall survival
S-CD/CD8-I4
S-CD/CD8-I1
S-CD/CD8-I3
S-CD/CD8-I2
S-CD/CD8-I0
p =0.060
Months after surgery
B
Overall survival
S-CD3/CD8-I4
S-CD3/CD8-I2&I3
S-CD3/CD8-I0&I1
p =0.059
Months after surgery
C
Overall survival
S-CD3/CD8-I4
S-CD3/CD8-I0 to I3
p =0.019
Months after surgery
D
Disease free survival
S-CD/CD8-I4
S-CD/CD8-I3
S-CD/CD8-I2
S-CD/CD8-I1
S-CD/CD8-I0
**
S-I4 vs. S-I0: p=0.004 **
p =0.079
Months after surgery
E
Disease free survival
S-CD3/CD8-I4
S-CD3/CD8-I2&I3
S-CD3/CD8-I0&I1
p =0.030
Months after surgery
F
Disease free survival
S-CD3/CD8-I4
S-CD3/CD8-I0 to I3
p =0.019
Months after surgery

Figure 8. Kaplan-Meier survival analysis with log-rank test of the S-CD3/CD8-I. A. Survival curves for the time of OS according to the S-CD3/CD8-I (No. of patients; S-CD3/CD8-I0, 32; S-CD3/CD8-I1, 29; S-CD3/CD8-I2, 27; S-CD3/CD8-I3, 22; S-CD3/CD8-I4, 33). **B.** Survival curves for OS of S-CD3/CD8-I0 and S-CD3/CD8-I1 (n = 61) vs. S-CD3/CD8-I2 and S-CD3/CD8-I3 (n = 49) vs. S-CD3/CD8-I4 (n = 33). **C.** Survival curves for OS of S-CD3/CD8-I0 to S-CD3/CD8-I3 (n = 110) vs. S-CD3/CD8-I4 (n = 33). **D.** Survival curves for the time of DFS according to the S-CD3/CD8-I (No. of patients; S-CD3/CD8-I0, 30; S-CD3/CD8-I1, 28; S-CD3/CD8-I2, 23; S-CD3/CD8-I3, 21; S-CD3/CD8-I4, 31) Patients who diagnosed as TNM stage IV were excluded in survival analysis for DFS. **Significant difference was observed for DFS duration between the patients with S-CD3/CD8-I4 and the patients with S-CD3/CD8-I0. **E.** Survival curves for DFS of S-CD3/CD8-I0 and S-CD3/CD8-I1 (n = 58) vs. S-CD3/CD8-I2 and S-CD3/CD8-I3 (n = 44) vs. S-CD3/CD8-I4 (n = 31). **F.** Survival curves for DFS of S-CD3/CD8-I0 to S-CD3/CD8-I3 (n = 102) vs. S-CD3/CD8-I4 (n = 31).

Abbreviations: S, stromal compartment, I, immunoscore, OS, overall survival; DFS, disease free survival

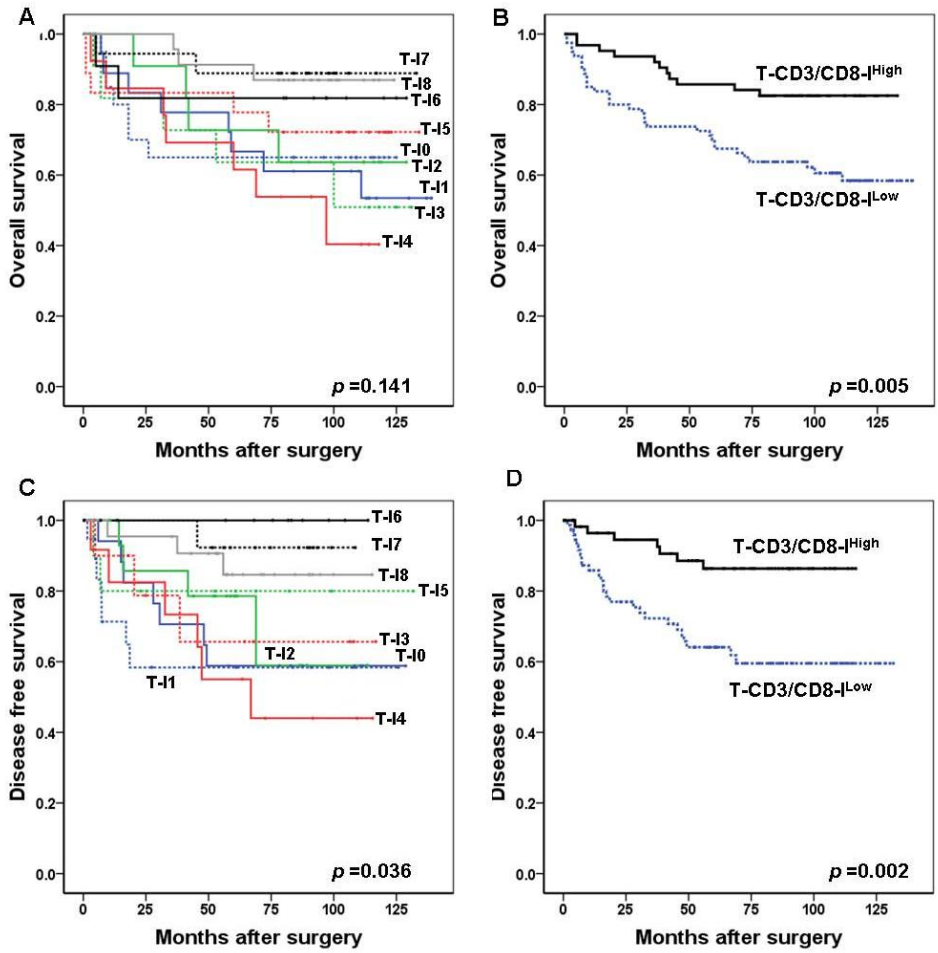

Figure 9. Kaplan-Meier survival analysis with log-rank test of the T-CD3/CD8-I. A. Survival curves for the time of OS according to the T-CD3/CD8-I (No. of patients; T-CD3/CD8-I0, 18; T-CD3/CD8-I1, 20; T-CD3/CD8-I2, 18; T-CD3/CD8-I3, 11; T-CD3/CD8-I4, 13; T-CD3/CD8-I5, 11; T-CD3/CD8-I6, 11; T-CD3/CD8-I7, 18; T-CD3/CD8-I8, 23). **B.** Survival curves for OS of T-CD3/CD8-I^{High} (n = 63) vs. T-CD3/CD8-I^{Low} (n = 80). **C.** Survival curves for the time of DFS according to the T-CD3/CD8-I (No. of patients; T-CD3/CD8-I0, 17; T-CD3/CD8-I1,

20; T-CD3/CD8-I2, 15; T-CD3/CD8-I3, 10; T-CD3/CD8-I4, 12; T-CD3/CD8-I5, 11; T-CD3/CD8-I6, 9; T-CD3/CD8-I7, 16; T-CD3/CD8-I8, 23). **D.** Survival curves for DFS of T-CD3/CD8-I^{High} (n = 59) vs. T-CD3/CD8-I^{Low} (n = 74).

Abbreviations: T, total compartment; I, immunoscore, OS, overall survival; DFS, disease free survival

Table 5. Association between Immunoscore and clinicopathologic characteristics

Parameters	*n*	E-CD3/CD8-I			S-CD3/CD8-I		
		0,1,2,3	4	*p*-value	0,1,2,3	4	*p*-value
Sex				0.780			0.246
Male	74	52 (52.5%)	22 (50%)		54 (49.1%)	20 (60.6%)	
Female	69	47 (47.5%)	22 (50%)		56 (50.9%)	13 (39.4%)	
Age (years)				>0.999			0.354
≤60	44	31 (31.3%)	13 (29.5%)		36 (32.7%)	8 (24.2%)	
>60	99	68 (68.7%)	31 (70.5%)		74 (67.3%)	25 (75.8%)	
Gross type				0.389			0.815
Polypoid	6	6 (6.1%)	0 (0%)		5 (4.5%)	1 (3%)	
Ulcerofungating	67	45 (45.5%)	22 (50%)		53 (48.2%)	14 (42.4%)	
Ulceroinfiltrative	55	37 (37.4%)	18 (40.9%)		40 (36.4%)	15 (45.5%)	
Diffuse	15	11 (11.1%)	4 (9.1%)		12 (10.9%)	3 (9.1%)	
Site				0.820			0.921
Cardia	4	3 (3%)	1 (2.3%)		3 (2.7%)	1 (3%)	
Fundus	1	1 (1%)	0 (0%)		1 (0.9%)	0 (0%)	
Body	43	28 (28.3%)	15 (34.1%)		34 (30.9%)	9 (27.3%)	
Antrum	95	67 (67.7%)	28 (63.6%)		72 (65.5%)	23 (69.7%)	
Tumor differentiation				0.517			0.440
WD/MD	61	44 (44.4%)	17 (38.6%)		45 (40.9%)	16 (48.5%)	
PD/Other	82	55 (55.6%)	27 (61.4%)		65 (59.1%)	17 (51.5%)	
Ming				0.799			0.486
Expanding	106	74 (74.7%)	32 (72.7%)		80 (72.7%)	26 (78.8%)	
Infiltrative	37	25 (25.3%)	12 (27.3%)		30 (27.3%)	7 (21.2%)	
Lauren				0.438			0.779
Intestinal	76	56 (56.6%)	20 (45.5%)		60 (54.5%)	16 (48.5%)	
Diffuse	41	27 (27.3%)	14 (31.8%)		30 (27.3%)	11 (33.3%)	
Mixed	26	16 (16.2%)	10 (22.7%)		20 (18.2%)	6 (18.2%)	
Lymphatic invasion				<0.001			0.002
Absent	50	24 (24.2%)	26 (59.1%)		31 (28.2%)	19 (57.6%)	
Present	93	75 (75.8%)	18 (40.9%)		79 (71.8%)	14 (42.4%)	
Vascular invasion				0.596			0.480
Absent	120	82 (82.8%)	38 (86.4%)		91 (82.7%)	29 (87.9%)	
Present	23	17 (17.2%)	6 (13.6%)		19 (17.3%)	4 (12.1%)	
Perineural invasion				0.004			0.314
Absent	89	54 (54.5%)	35 (79.5%)		66 (60%)	23 (69.7%)	

Present	54	45 (45.5%)	9 (20.5%)		44 (40%)	10 (30.3%)	
Tumor depth				0.151			0.653
T2/3	113	75 (75.8%)	38 (86.4%)		86 (78.2%)	27 (81.8%)	
T4	30	24 (24.2%)	6 (13.6%)		24 (21.8%)	6 (18.2%)	
LN metastasis				0.015			0.129
Absent	112	72 (72.7%)	40 (90.9%)		83 (75.5%)	29 (87.9%)	
Present	31	27 (27.3%)	4 (9.1%)		27 (24.5%)	4 (12.1%)	
AJCC Stage				0.012			0.171
I/II	85	52 (52.5%)	33 (75%)		62 (56.4%)	23 (69.7%)	
III/IV	58	47 (47.5%)	11 (25%)		48 (43.6%)	10 (30.3%)	
MLH1 expression				0.716			0.727
Absent	128	88 (88.9%)	40 (90.9%)		99 (90%)	29 (87.9%)	
Present	15	11 (11.1%)	4 (9.1%)		11 (10%)	4 (12.1%)	
MSH2 expression				0.225			0.319
Absent	8	4 (4%)	4 (9.1%)		5 (4.5%)	3 (9.1%)	
Present	135	95 (96%)	40 (90.9%)		105 (95.5%)	30 (90.9%)	

Abbreviations: E, epithelial compartment; S, stromal compartment; I, immunoscore; W/D, well differentiated; M/D, moderately differentiated; P/D, poorly differentiated; LN, lymph node; AJCC, American Joint Committee on Cancer; T-PD-L1, PD-L1 expression in tumor cells; I-PD-L1, PD-L1 expression in immune cells

Clinicopathological features associated with PD-L1 expression in MSI-H GCs.

PD-L1 positivity in tumor cells (T-PD-L1 (+)) and infiltrating immune cells (I-PD-L1 (+)) was detected in 33 (21.6%) and 43 (28.1%) of 153 MSI-H GCs, respectively. Double positivity in tumor cells and immune cells was observed in 18 cases (11.7%). The T-PD-L1 (+) phenotype was closely associated with a diffuse or mixed tumor type according to the Lauren classification (p = 0.033), less frequent lymphatic invasion (p = 0.002) and lower TNM stage (p = 0.030), compared with T-PD-L1 (-) phenotype (Table 6). I-PD-L1 (+) tumors were significantly correlated with the expanding type of GC according to the Ming classification (p = 0.042), less frequent lymphatic invasion (p = 0.001), less frequent perineural invasion (p = 0.019), less frequent LNM (p = 0.019) and lower TNM stage (p = 0.006) compared with I-PD-L1 (-) GCs. (Table 6).

Table 6. Associations between PD-L1 expression and clinicopathological characteristics.

Parameter	*n*	T-PD-L1[a]			I-PD-L1[a]		
		Negative	Positive	*p*-value	Negative	Positive	*p*-value
Sex				0.119			0.316
Male	74	53 (48.2)	21 (63.6)		49 (49.0)	25 (58.1)	
Female	69	57 (51.8)	12 (36.4)		51 (51.0)	18 (41.9)	
Age (years)				0.620			0.927
≤ 60	44	35 (31.8)	9 (27.3)		31 (31.0)	13 (30.2)	
> 60	99	75 (68.2)	24 (72.7)		69 (69.0)	30 (69.8)	
Gross type				0.125			0.191
Polypoid	6	5 (4.6)	1 (3.0)		5 (5.0)	1 (2.3)	
Ulcerofungating	67	46 (41.8)	21 (63.7)		41 (4.01)	26 (60.5)	
Ulceroinfiltrative	55	45 (40.9)	10 (30.3)		42 (42.0)	13 (30.2)	
Diffuse	15	14 (12.7)	1 (3.0)		12 (12.0)	3 (7.0)	
Site				0.600			0.200
Cardia	4	4 (3.6)	0 (0.0)		3 (3.0)	1 (2.3)	
Fundus	1	1 (0.9)	0 (0.0)		1 (1.0)	0 (0.0)	
Body	43	34 (30.9)	9 (27.3)		35 (35.0)	8 (18.6)	
Antrum	95	71 (64.6)	24 (72.7)		61 (61.0)	34 (79.1)	
Tumor differentiation				0.405			0.808
WD/MD	61	49 (44.5)	12 (36.4)		42 (42.0)	19 (44.2)	
PD/Other	82	61 (55.5)	21 (63.6)		58 (58.0)	24 (55.8)	
Ming				0.834			0.042
Expanding	37	28 (25.5)	9 (27.3)		21 (21.0)	16 (37.2)	
Infiltrative	106	82 (74.5)	24 (72.7)		79 (79.0)	27 (62.8)	
Lauren				0.033			0.304
Intestinal	76	65 (59.0)	11 (33.3)		55 (55.0)	21 (48.8)	
Diffuse	41	28 (25.5)	13 (39.4)		25 (25.0)	16 (37.2)	
Mixed	26	17 (15.5)	9 (27.3)		20 (20.0)	6 (14.0)	

Lymphatic invasion				0.002			0.001
Absent	50	31 (28.2)	19 (57.6)		26 (26.0)	24 (55.8)	
Present	93	79 (71.8)	14 (42.4)		74 (74.0)	19 (44.2)	
Vascular invasion				0.361			0.649
Absent	120	94 (85.5)	26 (78.8)		83 (83.0)	37 (86.0)	
Present	23	16 (14.5)	7 (21.2)		17 (17.0)	6 (14.0)	
Perineural invasion				0.550			0.019
Absent	89	67 (60.9)	22 (66.7)		56 (56.0)	33 (76.7)	
Present	54	43 (39.1)	11 (33.3)		44 (44.0)	10 (23.3)	
Tumor depth				0.653			0.072
T2/3	113	86 (78.2)	27 (81.8)		75 (75.0)	38 (88.4)	
T4	30	24 (21.8)	6 (18.2)		25 (25.0)	5 (11.6)	
LN metastasis				0.129			0.019
Absent	112	83 (75.5)	29 (87.9)		73 (73.0)	39 (90.7)	
Present	31	27 (24.5)	4 (12.1)		27 (27.0)	4 (9.3)	
AJCC stage				0.030			0.006
I/II	85	60 (54.5)	25 (75.8)		52 (52.0)	33 (76.7)	
III/IV	58	50 (45.5)	8 (24.2)		48 (48.0)	10 (23.3)	

Values are presented as the number (%).

[a]Included only for patients with available TMA data.

Abbreviations: T-PD-L1, PD-L1 expression in tumor cells; I-PD-L1, PD-L1 expression in immune cells; WD, well differentiated; MD, moderately differentiated; PD, poorly differentiated; LN, lymph node; AJCC, American Joint Committee on Cancer.; TMA, tissue microarray

Correlation between PD-L1 expression and immunoscore/TAM score

Compared with T-PD-L1 (-) tumors, T-PD-L1 (+) tumors were significantly associated with higher immunoscore and TAM score except for CD163+ TAM score ($p < 0.001$ for E-CD3/CD8-I; $p = 0.039$ for S-CD3/CD8-I; $p = 0.003$ for T-CD3/CD8-I; $p = 0.011$ for CD68+ TAM score; $p = 0.055$ for CD163+ TAM score) (Table 7). I-PD-L1 (+) tumors were significantly correlated with higher immunoscore and TAM score ($p < 0.001$ for E-CD3/CD8-I; $p < 0.001$ for S-CD3/CD8-I; $p < 0.001$ for T-CD3/CD8-I; $p < 0.001$ for CD68+ TAM score; $p = 0.005$ for CD163+ TAM score) (Table 7).

Table 7. Associations between PD-L1 expression and immunoscore and TAM score.

Parameters	*n*	T-PDL1[a]			I-PDL1[a]		
		Low	High	*p*-value	Low	High	*p*-value
E-CD3/CD8-I[a]				<0.001			<0.001
Score 0-3	99	85 (77.3%)	14 (42.4%)		79 (79%)	20 (46.5%)	
Score 4	44	25 (22.7%)	19 (57.6%)		21 (21%)	23 (53.5%)	
S-CD3/CD8-I[a]				0.039			<0.001
Score 0-3	110	89 (80.9%)	21 (63.6%)		86 (86%)	24 (55.8%)	
Score 4	33	21 (19.1%)	12 (36.4%)		14 (14%)	19 (44.2%)	
T-CD3/CD8-I[a]				0.003			<0.001
Low (score 0-4)	80	69 (62.7)	11 (33.3)		68 (68.0)	12 (27.9)	
High (score 5-8)	63	41 (37.3)	22 (66.7)		32 (32.0)	31 (72.1)	
CD68+ TAM score[a]				0.011			0.001
Score 0	21	19 (20.7%)	2 (6.9%)		19 (23.2%)	2 (5.1%)	
Score 1-3	79	62 (67.4%)	17 (58.6%)		55 (67.1%)	24 (61.5%)	
Score 4	21	11 (12%)	10 (34.5%)		8 (9.8%)	13 (33.3%)	
CD163+TAM score[a]				0.055			0.005
Score 0	21	19 (20.7%)	2 (6.9%)		19 (23.2%)	2 (5.1%)	
Score 1-3	81	62 (67.4%)	19 (65.5%)		55 (67.1%)	26 (66.7%)	
Score 4	19	11 (12%)	8 (27.6%)		8 (9.8%)	11 (28.2%)	

[a]Included only for patients with available TMA data.

Abbreviations: T-PD-L1, PD-L1 expression in tumor cells; I-PD-L1, PD-L1 expression in immune cells; E, epithelial compartment; S, stromal compartment; T, total compartment; I, immunoscore

Prognostic significance of T-PD-L1 and I-PD-L1 expression status in MSI-H GCs.

Although the tendency for a better survival outcome was observed in patients with T-PD-L1 (+) compared with those with T-PD-L1 (-) and in patients with I-PD-L1 (+) compared with those with I-PD-L1 (-), the expression status of T-PD-L1 and I-PD-L1 could not significantly discriminate the survival outcomes of these patients (p = 0.240 for T-PD-L1; p = 0.127 for I-PD-L1) (Figures 10A & 10B). Furthermore, a combination of T-PD-L1 and I-PD-L1 failed to demonstrate a survival difference among the four subgroups (T-PD-L1 (+)/I-PD-L1 (+) vs. T-PD-L1 (+)/I-PD-L1 (-) vs. T-PD-L1 (-)/I-PD-L1 (+) vs. T-PD-L1 (-)/I-PD-L1 (-)) (P = 0.308), despite the observation that patients in the T-PD-L1 (+)/I-PD-L1 (+) groups experienced the longest OS compared with the other groups (Figure 10C).

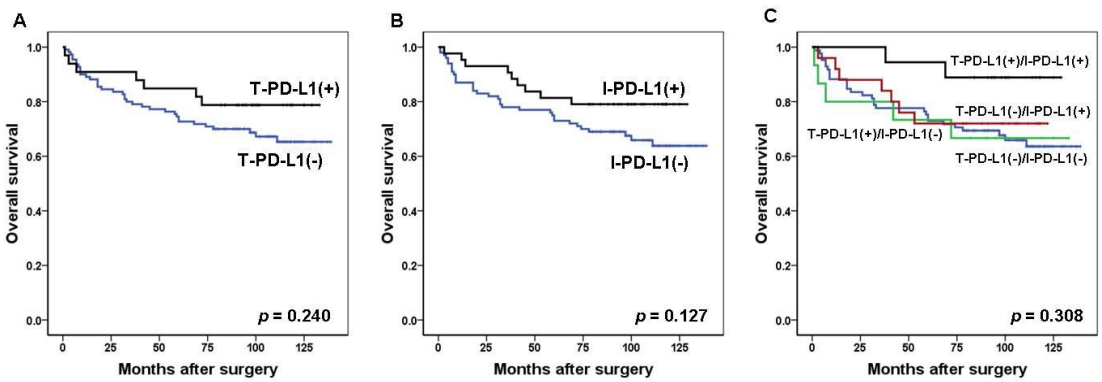

Figure 10. Kaplan-Meier survival analysis with log-rank test of the T-PD-L1 and I-PD-L1. A. Survival curves for the duration of OS according to PD-L1 expression in tumor cells (No. of patients; T-PD-L1 (+), 33; T-PD-L1 (-), 110). **B**, Survival curves for the duration of OS according to PD-L1 expression in immune cells (No. of patients; I-PD-L1 (+), 43; I-PD-L1 (-), 100). **C.** Survival curves for the duration of OS according to combined T-PD-L1 and I-PD-L1 expression status (No. of patients, T-PD-L1 (+)/I-PD-L1 (+), 18; T-PD-L1 (-)/I-PD-L1 (+), 25; T-PD-L1 (+)/I-PD-L1 (-), 15; T-PD-L1 (-)/I-PD-L1 (-), 85).

Abbreviations: T-PD-L1, PD-L1 expression in tumor cells, I-PD-L1, PD-L1 expression in stromal cells; OS, overall survival

Prognostic value of PD-L1 expression combined with the immunoscore in MSI-H GCs.

We then accounted for an integrated expression of T-PD-L1 and I-PD-L1 for the evaluation of comprehensive PD-L1 expression status in the tumor microenvironment. When the tumors were positive for either T-PD-L1 or I-PD-L1, they were classified into the "PD-L1 (+) group" while the remainders were classified into the "PD-L1 (-) group," According to the Kaplan-Meier survival analysis, no significant association was found between PD-L1 expression and OS (p = 0.242) (Figure 11A). To determine whether a differential prognostic effect of PD-L1 depended on the immunoscore, a combined analysis of the immunoscore and PD-L1 variables was performed. According to the Kaplan-Meier analysis, significant survival differences were observed among the four subgroups (p = 0.034) (Figure 11B). The best OS was observed in PD-L1 (+)/T-CD3/CD8-I^{High} patients, whereas, PD-L1 (+)/T-CD3/CD8-I^{Low} patients exhibited the worst OS. In particular, a distinct difference was noted in the OS between the patients with PD-L1 (+)/T-CD3/CD8-I^{High} and PD-L1 (+)/T-CD3/CD8-I^{Low} tumors (p = 0.011) (Figure 11B). A multivariate analysis with a Cox proportional hazard regression model that included lymphatic invasion, vascular invasion, perineural invasion, Ming classification, TNM stage, and the combination of PD-L1 expression and the immunoscore, which were significant factors in the univariate analysis, was performed. The combined status of PD-L1 expression and the immunoscore was an

independent and significant prognostic factor for OS in patients with MSI-H GC (p = 0.024) (Table 7), and notably, the patients with PD-L1 (+)/T-CD3/CD8-I^{High} tumors showed a significantly better clinical outcome than patients with PD-L1 (+)/T-CD3/CD8-I^{Low} tumors (p = 0.007) (Table 8).

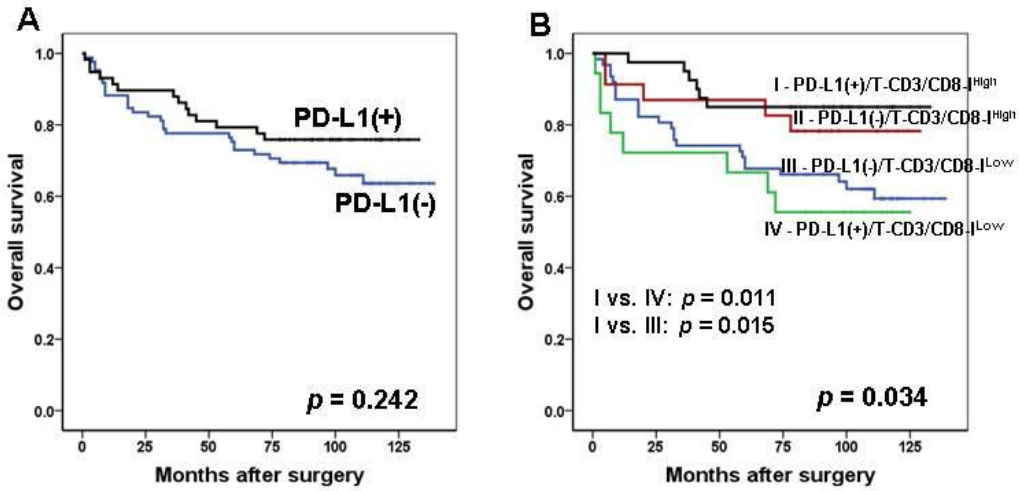

Figure 11. Kaplan-Meier survival analysis with log-rank test of the PD-L1 and PD-L1/immunoscore combination. **A.** Survival curves for the duration of OS according to PD-L1 expression status (No. of patients, PD-L1 (+), 58; PD-L1 (-), 85). **B.** Survival curves for the duration of OS according to the PD-L1/immunoscore combination (No. of patients, PD-L1 (+)/T-CD3/CD8-I^{High}, 40; PD-L1 (-)/T-CD3/CD8-I^{High}, 23; PD-L1 (+)/T-CD3/CD8-I^{Low}, 62; PD-L1 (-)/T-CD3/CD8-I^{Low}, 18).

Abbreviations: OS, overall survival; T, total compartment; I, immunoscore

Table 8. Univariate and multivariate analysis of OS among patients with MSI-H GCs.

Variable	Univariate analysis			Multivariate analysis[a]		
	n	HR (95% CI)	*p*-value	*n*	HR (95% CI)	*p*-value
Ming			0.004			0.076
Expanding	40	1 (Reference)		37	1 (Reference)	
Infiltrative	113	4.440 (1.589-12.408)		106	2.609 (0.906-7.514)	
Lymphatic invasion			0.004			0.337
Absent	54	1 (Reference)		50	1 (Reference)	
Present	99	3.084 (1.438-6.616)		93	1.531 (0.642-3.648)	
Vascular invasion			0.019			0.048
Absent	129	1 (Reference)		120	1 (Reference)	
Present	24	2.253 (1.143-4.441)		23	2.122 (1.007-4.472)	
Perineural invasion						0.724
Absent	97	1 (Reference)	0.001	89	1 (Reference)	
Present	56	2.754 (1.530-4.922)		54	1.124 (0.587-2.154)	
AJCC stage			<0.001			<0.001
I/II	92	1 (Reference)		85	1 (Reference)	
III/IV	61	7.975 (3.946-16.118)		58	4.868 (2.247-10.543)	
T-PD-L1 expression[a]			0.245		(-)	
Negative	110	1 (Reference)				
Positive	33	0.619 (0.275-1.391)				
I-PD-L1 expression[a]			0.133		(-)	
Negative	100	1 (Reference)				
Positive	43	0.569 (0.273-1.187)			(-)	
Combined PD-L1 expression[a]			0.246			
Negative	85	1 (Reference)				
Positive	58	0.685 (0.362-1.297)				
Combined PD-L1/Immunoscore[a]			0.048			0.024

PD-L1(+)/T-CD3/CD8-I^{High}	40	1 (Reference)		40	1 (Reference)	
PD-L1(-)/T-CD3/CD8-I^{High}	23	1.537 (0.469-5.036)	0.478	23	1.113 (0.323-3.841)	0.865
PD-L1(+)/T-CD3/CD8-I^{Low}	18	3.711 (1.287-10.701)	0.015	18	4.486 (1.494-13.469)	0.007
PD-L1(-)/T-CD3/CD8-I^{Low}	62	2.888 (1.180-7.071)	0.020	62	1.794 (0.703-4.576)	0.221

[a]Included only for patients with available TMA data.

Abbreviations: OS, overall survival; GCs, gastric cancers; MSI-H, microsatellite instability-high; HR, hazard ratio; CI, confidence interval; WD, well differentiated; MD, moderately differentiated; PD, poorly differentiated; T-PD-L1, PD-L1 expression in tumor cells; I-PD-L1, PD-L1 expression in immune cells; AJCC, American Joint Committee on Cancer; T, total compartment; I, immunoscore

The evaluation of TAM as a prognostic indicator

We divided the cohorts into 5 subgroups according to TAMs score to find out the prognostic role of CD68+ and CD163+ TAM in MSI-H GCs. However, in Kaplan-Meier survival analysis, the association between patients' outcome and the increase or decrease of TAM score did not follow the linear trend (Figure 12A & Figure 13A). In other words, patients with TAM score 0 showed the worst DFS, however, the score 4 subgroup showed the second worst DFS although statistical significance was not found (p = 0.115 for CD68+ TAM and p = 0.061 for CD163+ TAM). When the cases were reclassified into three subgroups (score 0 vs. score 4 vs. score 1 to 3), the score 4 was in the intermediate prognostic subgroups in both markers, with borderline significance (p = 0.115 for CD68+ and p = 0.053 for CD163+ TAM) (Figure 12B & Figure 13B). When the cases were dichotomized into high vs. low TAM score (score 0 vs. score 1-3), the patients with high CD163+ TAM score had statistically significant survival benefit for DFS, but those with high CD68+ TAM score showed marginally significant survival advantage for DFS (p = 0.072 for CD68+ TAM and 0.040 for CD163+ TAM) (Figure 12C & Figure 13C).

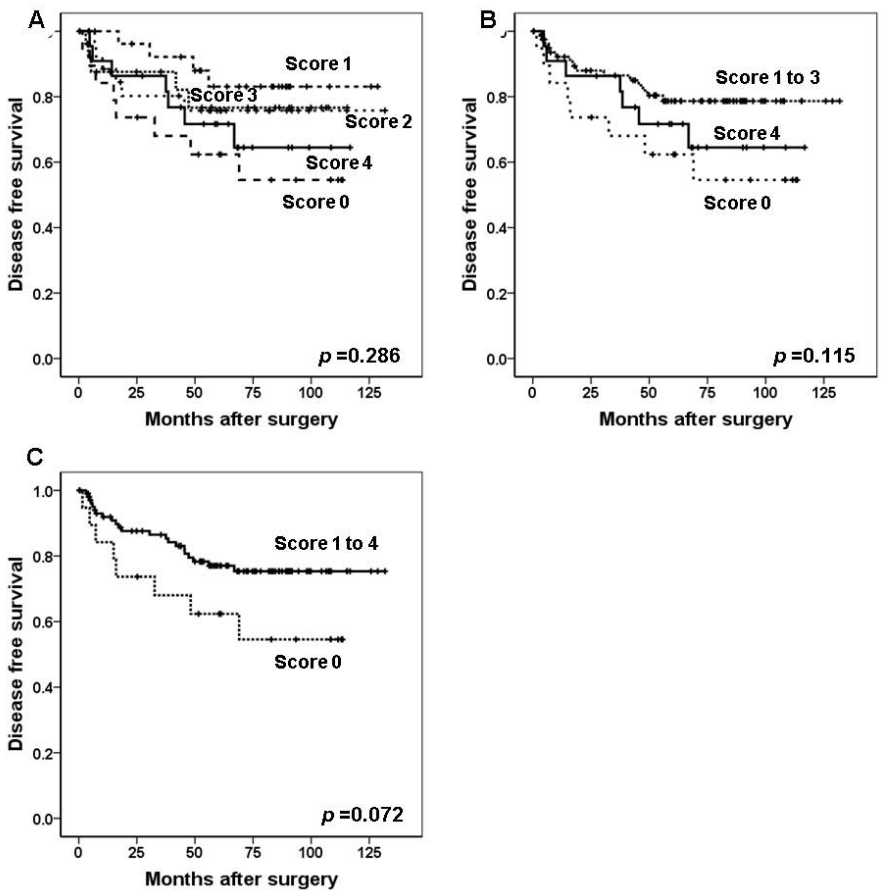

Figure 12. Kaplan-Meier survival analysis with log-rank test of the CD68+ TAM score. A. Survival curves for the time of DFS according to the TAM score (No. of patients; score 0, 20; score 1, 27; score 2, 28; score 3, 27; score 4, 22). Patients who diagnosed as TNM stage IV were excluded in survival analysis for DFS. **B.** Survival curves for DFS of TAM score 0 (n = 20) vs. TAM score 4 (n = 22) vs. TAM score 1 to 3 (n = 82). **C.** Survival curves for the time of DFS of TAM score 0 (n = 20) vs. TAM score 1 to 4 (n = 104).

Abbreviations: DFS, disease free survival

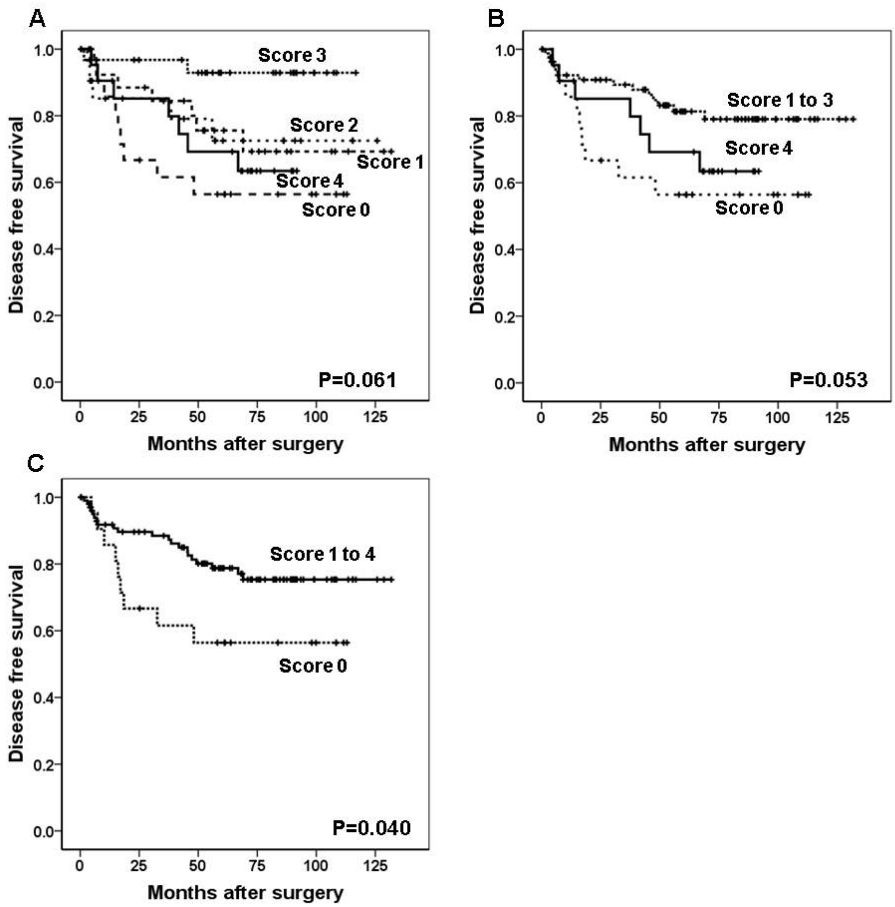

Figure 13. Kaplan-Meier survival analysis with log-rank test of the CD163+ TAM score. A. Survival curves for the time of DFS according to the TAM score (No. of patients; score 0, 21; score 1, 29; score 2, 21; score 3, 32; score 4, 21). Patients who diagnosed as TNM stage IV were excluded in survival analysis for DFS. **B.** Survival curves for DFS of TAM score 0 (n = 21) vs. TAM score 4 (n = 21) vs. TAM score 1 to 3 (n = 82). **C.** Survival curves for the time of DFS of TAM score 0 (n = 21) vs. TAM score 1 to 4 (n = 103).

Abbreviations: DFS, disease free survival

Multivariate survival analysis for OS and DFS in MSI-H GCs

To figure out the independent prognostic marker in MSI-H GCs, we conducted multivariate survival analysis that included Ming classification, lymphatic invasion, venous invasion, perineural invasion, AJCC stage, T-CD3/CD8-I, combined PD-L1 expression, CD68+ TAM score and CD163+ TAM score. In multivariate analysis with Cox proportional hazard regression model, AJCC stage ($p < 0.001$ for OS and DFS) and T-CD3/CD8-I were still independent predictors for OS and DFS ($p = 0.029$ for OS; $p = 0.034$ for DFS) (Table 9). Notably, positive PD-L1 expression was shown to be independent adverse prognostic marker for OS but not for DFS ($p = 0.034$ for OS; $p = 0.172$ for DFS). However, CD68+/CD163+ TAM score failed to be independent prognostic marker in MSI-H GCs ($p = 0.296$ for OS of CD68+ TAM score; $p = 0.058$ for DFS of CD68+ TAM score; $p = 0.080$ for OS of CD163+ TAM score; $p = 0.689$ for DFS of CD163+ TAM score).

Table 9. Multivariate Cox proportional hazard analysis of OS and DFS among patients with MSI-H GCs.

Variables		Overall survival		Disease free survival	
	n	Hazard ratio (95% CI)	*p*-value	Hazard ratio (95% CI)	*p*-value
Ming			0.075		0.147
Expanding	33	1		1	
Infiltrative	87	3.844 (0.875-16.889)		2.493 (0.725-8.570)	
Lymphatic invasion			0.960		0.966
Absent	45	1		1	
Present	75	0.973 (0.332-2.848)		1.022 (0.373-2.804)	
Vascular invasion			0.350		0.479
Absent	102	1		1	
Present	18	1.674 (0.568-4.930)		10470 (0.507-4.263)	
Perineural invasion			0.571		0.470
Absent	80	1		1	
Present	40	0.789 (0.347-1.792)		0.739 (0.326-1.678)	
AJCC stage			<0.001		<0.001
I/II	78	1		1	
III/IV	42	8.192 (2.713-24.733)		7.947 (2.724-23.187)	
T-CD3/CD8-I[a]			0.029		0.034
Low (score 0-4)	53	1		1	
High (score 1-5)	67	0.287 (0.093-0.883)		0.314 (0.107-0.917)	
Combined PD-L1 expression[a]			0.034		0.172
Negative	69	1		1	
Positive	51	2.763 (1.077-7.088)		1.912 (0.754-4.852)	
CD68+ TAM score[a]			0.296		0.058
Score 0	20	1		1	
Score 1-4	100	0.499 (0.136-1.836)		0.291 (0.081-1.040)	
CD163+ TAM score[a]			0.080		0.689
Score 0	21	1		1	
Score 1-4	99	0.389 (0.135-1.119)		0.800 (0.268-2.390)	

[a]Included only for patients with available TMA data.

Abbreviations: OS, overall survival; DFS, disease free survival; CI, confidence interval; AJCC, American Joint Committee on Cancer; T; total compartment; I, immunoscore

DISCUSSION

Increasing evidences of the studies have revealed that the presence of inflammatory cells within tumor microenvironment is associated with improved clinical outcome and increased response to chemotherapy and radiotherapy [40]. The correlation of the high density of TILs and favorable prognosis have been demonstrated in various tissues and tumor types, including colorectal [6], breast [41] and prostatic [42] and esophageal cancers [43] as well as malignant melanoma [44]. Among many T lymphocytes subpopulations, CD3, CD8 and CD45RO were most frequently used for markers of immunohistochemistry [10]. For comprehensive estimation of prognostic immune parameters, the concept of "immune contexture" was applied, which is defined by the type, density, functional orientation and location of the immune cells within distinct tumor regions [40,45]. To improve the utility of estimation of the immune cell infiltration in clinical setting, several researchers established the "immunoscore" that is based on numeration of two lymphocytes population, representatively CD3+ and CD8+ T lymphocytes, in tumor center (TC) and invasive front (IF) in CRCs [40]. In our study, we found that high immnoscore was correlated with prolonged OS and DFS in both tumor compartments (E and S) and high immunoscore in both stromal and epithelial compartment (T-CD3/C8-I^{High}) was an independent good prognostic indicator in MSI-H GCs. These finding supports the idea that immunoscore is a reliable tool for predicting patients' survival in MIS-H GCs. In addition, it can be inferred that relatively good prognosis of the patient with MIS-H tumors, to some extent, is

attributed to the increased numbers of TIL. These argument is supported by Galon et al' study which have demonstrated that there was no significant survival difference between CRCs patients with MSS having high immune-related gene expression and those with MSI [46]. They insisted that, in predicting patients' survival, immunoscore is more stronger than MSI. In this study, infiltrating immune cells were separately evaluated in two distinct compartments (epithelial and stromal compartment) for more objective results. This decision was based on the fact that the distribution of TIL differs between the two compartments and the ratio of the stroma and epithelium varies in the cores of TMA between cases [41, 47].

The correlation between PD-L1 expression and microsatellite instability has been demonstrated in several studies. Recently, a phase II clinical trial showed that anti-PD-1/PD-L1 therapy can be beneficial to patients who have advanced stage MSI-H colorectal cancer (CRC) [17]. The correlation between MSI-H cancers and high PD-L1 expression is logical given that MSI-H tumors have an increased number of tumor infiltrating immune cells, particularly Th1 and cytotoxic T cells, as well as a higher expression of immune checkpoint molecules [18]. This phenomenon is due to many immunogenic neo-antigens that are produced by frequent frameshift mutations in MSI-H tumors. However, not all MSI-GCs harbor dense infiltration of TILs in the tumor microenvironment, and not all express a high level of PD-L1. Instead, a wide spectrum of TIL density and PD-L1 expression may exist within MSI-H GCs. Because MSI-H GCs are a relatively homogenous group in terms of

molecular carcinogenesis, they might be good sources through which to assess the prognostic value of PD-L1 expression and its relationship to the tumor microenvironment.

In our study, PD-L1 expression was observed in tumor cells (n = 33, 21.6%) as well as in infiltrating immune cells (n = 43, 28.1%), and a substantial number of tumors showed co-expression of PD-L1 in both tumor cells and immune cells (n = 18, 11.7%). Although the biological meaning of these differential expression patterns is elusive, they are likely governed by combined innate (intrinsic) and adaptive cellular (extrinsic) factors within the tumor microenvironment [48]. The expression of PD-L1 has been reported to be regulated by intrinsic and extrinsic mechanisms in the tumor microenvironment [49]. The extrinsic induction is basically dependent on the pro-inflammatory cytokine interferon gamma (IFN-γ), which is secreted by CD8+ cytotoxic T cells; consequently, this induces the expression and transcription of PD-L1 on the surface of tumor cells and infiltrating immune cells [50]. In contrast, the intrinsic induction of PD-L1 on the surface of tumor cells is mediated by constitutive oncogenic and transcriptional pathways, such as the PI3K and mTOR pathways in non-small cell lung cancer and the EGFR-MAP kinase pathway in breast cancer [49]. In our study, a significant correlation was observed between T-PD-L1 expression and a high immunoscore. These findings likely reflect that PD-L1 expression in tumor cells is mainly controlled by an extrinsic (adaptive immune) mechanism rather than an intrinsic pathway in MSI-H GCs. In this regard, the results of the study by Derks *et al*.

corresponded with our results in that MSI-H GCs exhibited expression of high IFN-γ response genes compared with genetically stable GCs according to a gene set enrichment analysis [50]. However, our results contrast with those of the study by Kim *et al*. [51]. They showed that PD-L1 expression in tumor cells was not associated with the densities of immune cells (CD3+, CD4+, CD8+, and PD-1+ cells) in 243 cases of GC. The discrepancy between the two studies can be attributed to the heterogeneity present in the study by Kim *et al*.'s group, as their study might have contained MSS/MSI-L GCs in excess of MSI-H GCs. The discrepancy also reflects a fundamental difference in the expression mechanisms of PD-L1 on tumor cells between MSS/MSI-L and MSI-H GCs. In addition, a more significant correlation was noted between I-PD-L1 expression and a high immunoscore. These findings seem plausible considering that CD3+ TILs, CD8+ TILs, and PD-L1-expressing immune cells are inherent components of the adaptive immune system, which is robustly activated in MSI-H GCs.

Some results in regards to the prognostic value of PD-L1 expression in GCs are conflicting. Although most previous studies revealed a correlation between high PD-L1 expression and reduced survival rate [52, 53], several recent studies revealed that high PD-L1 expression had a positive impact on patient survival in GCs [20, 51, 54]. In our study, no significant survival difference was observed between the PD-L1 (+) and PD-L1 (-) groups. However, a combined survival analysis of PD-L1 expression and the immunoscore revealed four distinct subgroups with statistically significant differences in the OS. Notably, the PD-L1

(+)/T-CD3/CD8-I^{Low} showed the worst prognosis, and the PD-L1 (+)/T-CD3/CD8-I^{High} group showed the best prognosis. Based on previous research, PD-L1 (+)/T-CD3/CD8-I^{High} refers to the group in which the adaptive immune system is primarily activated via the PD-l/PD-L1 signaling pathway, whereas the PD-L1 (+)/T-CD3/CD8-I^{Low} group is considered to be associated with intrinsic induction of PD-L1 by an oncogenic pathway regardless of IFN-γ expression [49]. The reason why the PD-L1 (+)/T-CD3/CD8-I^{High} subgroup has the most favorable prognosis, contrary to our expectations, might be because of a compensatory up-regulation of PD-L1 mediated by an ongoing overloaded antitumor immune response, rather than because of tumor immune evasion itself [55, 56]. This indicates that anti-tumor cytotoxic T cells and their counteractive molecules such as PD-L1 are simultaneously activated in highly immunogenic conditions in which TILs are abundant. In addition, the prognostic role of PD-L1 might be influenced by the tension state of complex immune contextures. However, according to our findings, it is noteworthy that intrinsic PD-L1 expression (PD-L1 (+)/T-CD3/CD8-I^{Low}), is most harmful to patients with MSI-H GC. The mechanism by which PD-L1 expression through the intrinsic pathway is associated with the most aggressive behavior has not been clearly elucidated. Moreover, no relevant data have been obtained as to whether the patients in this group might also benefit from anti-PD-1/PD-L1 therapy. Using larger-scale cohorts of GC patients, future studies should clarify the role of the combination of PD-L1 expression and the presence of TILs in

the tumor microenvironment as a putative prognostic indicator and as a predictive biomarker for the application of anti-PD-1/PD-L1 therapy.

The correlation between the high density of TILs and a favorable prognosis has been demonstrated in various tissues and tumor types, including colorectal [39], breast [57], and prostate [58] cancers. In addition to its role as a prognostic marker, the presence of TILs is also recognized as a predictive biomarker for anti-PD-1/PD-L1 therapy. Tumeh *et al*. reported that, in patients with stage III malignant melanoma, the most predictive marker of clinical response to PD-1 blockade was the density of CD8+ TILs in the TC and IF and was not PD-1 or PD-L1 expression itself in patients [59]. Considering this, a larger number of patients with MSI-H GC might be potential candidates for anti-PD-1/PD-L1 therapy regardless of their PD-1 or PD-L1 expression status. For more efficient use of anti-PD-1/PD-L1 antibodies in GC patients, a standardized set of criteria is required regarding several factors such as the types of antibodies and staining methods to be used, and the cut-off level for positivity of PD-L1 expression in terms of both intensity and extent (in non-small cell lung cancer, patients with tumors in which at least 50% of tumor cells expressed PD-L1 were candidates for second line treatment of pembrolizumab [60]). Another factor to consider is the cell type that will be evaluated among tumor cells and infiltrating immune cells (in patients with metastatic urinary bladder cancer, PD-L1 expression in tumor infiltrating immune cells was proven to have predictive value for anti-PD-L1 antibody treatment [61]).

In the present study, we analyzed the prognostic implication of CD68+ or CD163+ TAMs in MSI-H GCs. In the tumor microenvironment, macrophages constitute major components of tumor-infiltrating leukocytes and affect tumor cells by releasing many chemical substances. Two phenotypic subtypes of TAMs–M1 and M2 macrophages–have been reported to have opposite roles in tumor progression. M2 macrophages are thought to have tumor promoting functions whereas M1 macrophages have shown a protective role in tumorigenesis. As TAMs are more closely linked to M2 type rather than M1 type macrophages, many studies have demonstrated that high levels of TAMs are associated with poor clinical outcome in human cancers, including breast, ovary, lung and endometrial cancers [24, 27–30]. However, in GCs, conflicting results have been reported [62].

CD68 has been used as a marker of overall infiltrated TAM covering a majority of functionally activated macrophages regardless of their polarization state in many studies. Wang et al.'s study showed that intra-tumoral infiltrating CD68+ TAMs are independent good prognostic factors in GCs [36]. In contrast, Wu et al.'s study demonstrated that CD68+ TAMs promote angiogenesis and lymphangiogenesis of GCs [63]. However, Zhang et al.'s study showed that CD68+ TAMs in GCs have no significant association with overall survival [64]. In our study, CD68+ TAMs were found to have no prognostic impact on DFS in MSI-H GCs. Along with CD68+ TAMs, recent studies have focused on the specific role of each subset of TAMs by discriminating the M1 and M2 phenotypes.

CD163 is a member of histiocyte/macrophage-associated scavenger receptor [65]. Although the expression of CD163 has been reported in cells other than M2 macrophages, such as dendritic cells, CD163 can be a useful marker to distinguish M2 macrophages from other subsets. Many studies have demonstrated an adverse prognostic effect of M2 macrophages on clinical outcome in GCs [64, 65]. However, a beneficial role of M2 macrophages on prognosis has been reported in hollow viscus tumors, e.g., CRCs. Algar et al.'s study concluded that the type and location of tumor infiltrating macrophages contribute to the clinical behavior of CRCs in a stage-specific manner, by demonstrating that in stage III CRCs, a high number of M2 macrophages in the peritumoral area correlated with prolonged cancer-specific survival time [66]. However, in a more advanced stage, a reverse correlation was observed. In addition, Edin et al.'s study also showed that increased infiltration of M1 or M2 type macrophages at the invasive front was associated with significantly improved cancer-related survival in CRCs [33]. Our study demonstrated that low density of CD163+ TAMs (score 0) was significantly correlated with prolonged DFS compared with the remainders (score 1 to score 4). However, the patients with TAM score 4 showed the tendency to have second worst DFS in MSI-H GCs. Based on these results, it can be inferred that the exaggerated number of TILs which occur as a consequence of MSI seems to exert considerable influence on prognostic role of CD163+ TAMs in MSI-H GCs, in spite of the original tumor-promoting function of CD163+ TAMs. The positive correlation between CD3+/CD8+ TILs and CD163+ TAMs in each compartment

(E and S) was shown in our data except for the correlation between stromal CD3+ TILs and CD163+ TAMs. TAMs and TILs are considered to interact on each other in the tumor microenvironment and the prognostic effect can be determined in proportional balance of both TAMs and TILs in MSI-H GCs. The parallel analysis in other molecular subtypes, including MSI- and EBV-negative GCs or EBV-positive GCs, is required for figuring out the prognostic role of balanced high infiltrations of both TAMs and TILs and the exact role of MSI on functional differentiation of CD163+ TAMs. Moreover, M2 macrophages are thought to be involved in immunoregulation by inducing the skewing of TILs toward a more regulatory phenotype [22, 67] which have protective role on tumor development in MSI-H GCs according to our previous study [68].

In conclusion, our study revealed that the immunoscore using CD3+ and CD8+ T lymphocytes subpopulation is a reliable methodology to predict the clinical outcome of MIS-H GC patients and high immunoscore is positively correlated with PD-L1 expression in tumor cells and immune cells in MSI-H GCs. We also demonstrated that PD-L1 expression is mainly induced by adaptive immune resistant mechanism in MSI-H GCs. Furthermore, immunoscore can be a relevant regulator in determining the prognostic role of PD-L1 expression in MSI-H GCs. Although, the prognostic role of TAM was not entirely elucidated, TILs and TAMs are considered to be influenced by each other and the prognostic effect can be determined in proportional balance of both TAMs and TILs in MSI-H GCs.

REFERENCES

1. Ferlay J, Shin HR, Bray F, et al. (2010) Estimates of worldwide burden of cancer in 2008: GLOBOCAN 2008. Int J Cancer. 127:2893--2917.

2. Shokal U, Sharma PC (2012) Implication of microsatellite instability in human gastric cancers. Indian J Med Res. 135:599-613.

3. Choi YY, Bae JM, An JY, et al. (2014) Is microsatellite instability a prognostic marker in gastric cancer? A systematic review with meta-analysis. J Surg Oncol. 110:129-135.

4. Kim H, An JY, Noh SH, et al. High microsatellite instability predicts good prognosis in intestinal-type gastric cancers. Journal of gastroenterology and hepatology. 2011;26(3):585-92.

5. Angell H, Galon J. From the immune contexture to the Immunoscore: the role of prognostic and predictive immune markers in cancer. Current opinion in immunology. 2013;25(2):261-7.

6. Anitei MG, Zeitoun G, Mlecnik B, et al. Prognostic and predictive values of the immunoscore in patients with rectal cancer. Clinical cancer research : an official journal of the American Association for Cancer Research. 2014;20(7):1891-9.

7. Galon J, Fridman WH, Pages F. The adaptive immunologic microenvironment in colorectal cancer: a novel perspective. Cancer research. 2007;67(5):1883-6.

8. Gabrielson A, Wu Y, Wang H, et al. Intratumoral CD3 and CD8 T-cell Densities Associated with Relapse-Free Survival in HCC. Cancer immunology research. 2016;4(5):419-30.

9. Fridman WH, Pages F, Sautes-Fridman C, et al. The immune contexture in human tumours: impact on clinical outcome. Nature reviews Cancer. 2012;12(4):298-306.

10. Galon J, Pages F, Marincola FM, et al. Cancer classification using the Immunoscore: a worldwide task force. Journal of translational medicine. 2012;10:205.

11. Spranger S, Spaapen RM, Zha Y, et al. Up-regulation of PD-L1, IDO, and T(regs) in the melanoma tumor microenvironment is driven by CD8(+) T cells. Science translational medicine. 2013;5(200):200ra116.

12. Gabrielson A, Wu Y, Wang H, et al. Intratumoral CD3 and CD8 T-cell Densities Associated with Relapse-Free Survival in HCC. Cancer Immunol Res. 2016; 4(5):419-430.

13. Spranger S, Spaapen RM, Zha Y, et al. Up-regulation of PD-L1, IDO, and T(regs) in the melanoma tumor microenvironment is driven by CD8(+) T cells. Sci Transl Med. 2013; 5(200):200ra116.

14. Topalian SL, Hodi FS, Brahmer JR, et al. Safety, activity, and immune correlates of anti-PD-1 antibody in cancer. N Engl J Med. 2012; 366(26):2443-2454.

15. de Guillebon E, Roussille P, Frouin E, et al. Anti program death-1/anti program death-ligand 1 in digestive cancers. World J Gastrointest Oncol. 2015; 7(8):95-101.

16. Muro K, Chung HC, Shankaran V, et al. Pembrolizumab for patients with PD-L1-positive advanced gastric cancer (KEYNOTE-012): a multicentre, open-label, phase 1b trial. Lancet Oncol. 2016; 17(6):717-726.

17. Le DT, Uram JN, Wang H, et al. PD-1 Blockade in Tumors with Mismatch-Repair Deficiency. N Engl J Med. 2015; 372(26):2509-2520.

18. Mlecnik B, Bindea G, Angell HK, et al. Integrative Analyses of Colorectal Cancer Show Immunoscore Is a Stronger Predictor of Patient Survival Than Microsatellite Instability. Immunity. 2016; 44(3):698-711.

19. Kawazoe A, Kuwata T, Kuboki Y, et al. Clinicopathological features of programmed death ligand 1 expression with tumor-infiltrating lymphocyte, mismatch repair, and Epstein-Barr virus status in a large cohort of gastric cancer patients. 2016.

20. Boger C, Behrens HM, Mathiak M, et al. PD-L1 is an independent prognostic predictor in gastric cancer of Western patients. Oncotarget. 2016; 7(17):24269-24283.

21. Llosa NJ, Cruise M, Tam A, et al. The vigorous immune microenvironment of microsatellite instable colon cancer is balanced by multiple counter-inhibitory checkpoints. Cancer Discov. 2015; 5(1):43-51.

22. Biswas SK, Allavena P, Mantovani A. Tumor-associated macrophages: functional diversity, clinical significance, and open questions. Semin Immunopathol. 2013; 35:585-600.

23. Ramanathan S, Jagannathan N. Tumor associated macrophage: a review on the phenotypes, traits and functions. Iran J Cancer Prev. 2014; 7:1-8.

24. Reinartz S, Schumann T, Finkernagel F, et al. Mixed-polarization phenotype of ascites-associated macrophages in human ovarian carcinoma: correlation of CD163 expression, cytokine levels and early relapse. Int J Cancer. 2014; 134:32-42.

25. Tham M, Tan KW, Keeble J, et al. Melanoma-initiating cells exploit M2 macrophage TGF-beta and arginase pathway for survival and proliferation. Oncotarget. 2014; 5:12027-12042.

26. Kumagai S, Marumo S, Shoji T, et al. Prognostic impact of preoperative monocyte counts in patients with resected lung adenocarcinoma. Lung Cancer. 2014; 85:457464.
27. Pei BX, Sun BS, Zhang ZF, et al. Interstitial tumor-associated macrophages combined with tumor-derived colony-stimulating factor-1 and interleukin-6, a novel prognostic biomarker in non-small cell lung cancer. J Thorac Cardiovasc Surg. 2014; 148:1208-1216.e2.
28. Kubler K, Ayub TH, Weber SK, et al. Prognostic significance of tumor-associated macrophages in endometrial adenocarcinoma. Gynecol Oncol. 2014; 135:176-183
29. Zhang Y, Cheng S, Zhang M, et al. High-infiltration of tumor-associated macrophages predicts unfavorable clinical outcome for node-negative breast cancer. PLoS One. 2013; 8:e76147.
30. Yuan ZY, Luo RZ, Peng RJ, et al. High infiltration of tumor-associated macrophages in triple-negative breast cancer is associated with a higher risk of distant metastasis. Onco Targets Ther. 2014; 7:1475-1480.
31. Behnes CL, Bremmer F, Hemmerlein B, et al. Tumor-associated macrophages are involved in tumor progression in papillary renal cell carcinoma. Virchows Arch. 2014; 464:191-196.
32. Dannenmann SR, Thielicke J, Stockli M, et al. Tumor-associated macrophages subvert T-cell function and correlate with reduced survival in clear cell renal cell carcinoma. Oncoimmunology. 2013; 2:e23562.
33. Edin S, Wikberg ML, Dahlin AM, et al. The distribution of macrophages with a M1 or M2 phenotype in relation to prognosis and the molecular characteristics of colorectal

cancer. PLoS One. 2012; 7:e47045.

34. Erreni M, Mantovani A, Allavena P. Tumor-associated Macrophages (TAM) and Inflammation in Colorectal Cancer. Cancer Microenviron. 2011; 4:141-154.

35. Forssell J, Oberg A, Henriksson ML, et al. High macrophage infiltration along the tumor front correlates with improved survival in colon cancer. Clin Cancer Res 2007; 13:1472-1479.

36. Wang B, Xu D, Yu X, et al. Association of intra-tumoral infiltrating macrophages and regulatory T cells is an independent prognostic factor in gastric cancer after radical resection. Ann Surg Oncol. 2011; 18:2585-2593.

37. Darb-Esfahani S, Kunze CA, Kulbe H, et al. Prognostic impact of programmed cell death-1 (PD-1) and PD-ligand 1 (PD-L1) expression in cancer cells and tumor-infiltrating lymphocytes in ovarian high grade serous carcinoma. Oncotarget. 2016;7(2):1486-99.

38. Angell H and Galon J. From the immune contexture to the Immunoscore: the role of prognostic and predictive immune markers in cancer. Curr Opin Immunol. 2013; 25(2):261-267.

39. Anitei MG, Zeitoun G, Mlecnik B, et al. Prognostic and predictive values of the immunoscore in patients with rectal cancer. Clin Cancer Res. 2014; 20(7):1891-1899.

40. Kirilovsky A, Marliot F, El Sissy C, et al. Rational bases for the use of the Immunoscore in routine clinical settings as a prognostic and predictive biomarker in cancer patients. International immunology. 2016;28(8):373-82.

41. Mahmoud SM, Paish EC, Powe DG, et al. Tumor-infiltrating CD8+ lymphocytes

predict clinical outcome in breast cancer. Journal of clinical oncology : official journal of the American Society of Clinical Oncology. 2011;29(15):1949-55.

42. Karja V, Aaltomaa S, Lipponen P, et al. Tumour-infiltrating lymphocytes: A prognostic factor of PSA-free survival in patients with local prostate carcinoma treated by radical prostatectomy. Anticancer research. 2005;25(6c):4435-8.

43. Schumacher K, Haensch W, Roefzaad C, et al. Prognostic significance of activated CD8(+) T cell infiltrations within esophageal carcinomas. Cancer research. 2001;61(10):3932-6.

44. Piras F, Colombari R, Minerba L, et al. The predictive value of CD8, CD4, CD68, and human leukocyte antigen-D-related cells in the prognosis of cutaneous malignant melanoma with vertical growth phase. Cancer. 2005;104(6):1246-54.

45. Galon J, Costes A, Sanchez-Cabo F, et al. Type, density, and location of immune cells within human colorectal tumors predict clinical outcome. Science (New York, NY). 2006;313(5795):1960-4.

46. Mlecnik B, Bindea G, Angell HK, et al. Integrative Analyses of Colorectal Cancer Show Immunoscore Is a Stronger Predictor of Patient Survival Than Microsatellite Instability. Immunity. 2016;44(3):698-711.

47. Kyndi M, Sorensen FB, Knudsen H, et al. Tissue microarrays compared with whole sections and biochemical analyses. A subgroup analysis of DBCG 82 b&c. Acta oncologica (Stockholm, Sweden). 2008;47(4):591-9.

48. Taube JM, Klein A, Brahmer JR, et al. Association of PD-1, PD-1 ligands, and other features of the tumor immune microenvironment with response to anti-PD-1 therapy.

Clin Cancer Res. 2014; 20(19):5064-5074.

49. Sanmamed MF and Chen L. Inducible expression of B7-H1 (PD-L1) and its selective role in tumor site immune modulation. Cancer J. 2014; 20(4):256-261.

50. Derks S, Liao X, Chiaravalli AM, et al. Abundant PD-L1 expression in Epstein-Barr Virus-infected gastric cancers. Oncotarget. 2016; 7(22):32925-32932.

51. Kim JW, Nam KH, Ahn SH, et al. Prognostic implications of immunosuppressive protein expression in tumors as well as immune cell infiltration within the tumor microenvironment in gastric cancer. Gastric Cancer. 2016; 19(1):42-52.

52. Thompson ED, Zahurak M, Murphy A, et al. Patterns of PD-L1 expression and CD8 T cell infiltration in gastric adenocarcinomas and associated immune stroma. Gut. 2016.

53. Geng Y, Wang H, Lu C, et al. Expression of costimulatory molecules B7-H1, B7-H4 and Foxp3+ Tregs in gastric cancer and its clinical significance. Int J Clin Oncol. 2015; 20(2):273-281.

54. Cho J, Lee J, Bang H, et al. Programmed cell death-ligand 1 expression predicts survival in patients with gastric carcinoma with microsatellite instability. Oncotarget. 2017.

55. Darb-Esfahani S, Kunze CA, Kulbe H, et al. Prognostic impact of programmed cell death-1 (PD-1) and PD-ligand 1 (PD-L1) expression in cancer cells and tumor-infiltrating lymphocytes in ovarian high grade serous carcinoma. Oncotarget. 2016; 7(2):1486-1499.

56. Schalper KA, Velcheti V, Carvajal D, et al. In situ tumor PD-L1 mRNA expression is associated with increased TILs and better outcome in breast carcinomas. Clin Cancer Res.

2014; 20(10):2773-2782.

57. Mahmoud SM, Paish EC, Powe DG, et al. Tumor-infiltrating CD8+ lymphocytes predict clinical outcome in breast cancer. J Clin Oncol. 2011; 29(15):1949-1955.

58. Karja V, Aaltomaa S, Lipponen P, et al. Tumour-infiltrating lymphocytes: A prognostic factor of PSA-free survival in patients with local prostate carcinoma treated by radical prostatectomy. Anticancer Res. 2005; 25(6c):4435-4438.

59. Tumeh PC, Harview CL, Yearley JH, et al. PD-1 blockade induces responses by inhibiting adaptive immune resistance. Nature. 2014; 515(7528):568-571.

60. Herbst RS, Baas P, Kim DW, et al. Pembrolizumab versus docetaxel for previously treated, PD-L1-positive, advanced non-small-cell lung cancer (KEYNOTE-010): a randomised controlled trial. Lancet. 2016; 387(10027):1540-1550.

61. Powles T, Eder JP, Fine GD, et al. MPDL3280A (anti-PD-L1) treatment leads to clinical activity in metastatic bladder cancer. Nature. 2014; 515(7528):558-562.

62. Komohara Y, Jinushi M, Takeya M. Clinical significance of macrophage heterogeneity in human malignant tumors. Cancer Sci. 2014; 105:1-8.

63. Wu H, Xu JB, He YL, et al. Tumor-associated macrophages promote angiogenesis and lymphangiogenesis of gastric cancer. J Surg Oncol. 2012; 106:462-468.

64. Zhang H, Wang X, Shen Z, et al. Infiltration of diametrically polarized macrophages predicts overall survival of patients with gastric cancer after surgical resection. Gastric Cancer. 2014; 18:740-750

65. Nam SJ, Go H, Paik JH, et al. An increase of M2 macrophages predicts poor prognosis in patients with diffuse large B-cell lymphoma treated with rituximab,

cyclophosphamide, doxorubicin, vincristine and prednisone. Leuk Lymphoma. 2014; 55:2466-2476.

66. Algars A, Irjala H, Vaittinen S, et al. Type and location of tumor-infiltrating macrophages and lymphatic vessels predict survival of colorectal cancer patients. Int J Cancer. 2012; 131:864--873.

67. Subhra K Biswas, Alberto Mantovani. Macrophage plasticity and interaction with lymphocyte subsets: cancer as a paradigm. Nat Immunol. 2010; 11:889-896.

68. Kim KJ, Lee KS, Cho HJ, et al. Prognostic implications of tumor-infiltrating FoxP3+ regulatory T cells and CD8+ cytotoxic T cells in microsatellite-unstable gastric cancers. Hum Pathol. 2014; 45:285-293.

국문 초록

김 경 주

의학과 병리학전공

서울대학교 의과대학

서론: 현미부수체불안정성 위암은 위암의 약 10% 정도를 차지하고, 많은 수의 틀이동성변이를 가짐으로써 현미부수체안정성 위암에 비해 높의 밀도의 종양내침윤림프구와 종양관련대식구를 가지고, PD-L1을 비롯한 항면역검문 단백의 발현 또한 높은 것으로 알려져 있다.

방법: 이번 연구에서는 서울대학교 병원에서 외과적 절제가 시행된 153례의 현미부수체불안정성 진행성 위암 조직을 대상으로 조직미세배열의 방법을 사용하여 종양내침윤림프구, 종양관련대식구 및 PD-L1이 환자의 예후에 미치는 영향에 대해 밝히고, 이들 간의 상관관계를 밝히고자 하였다. 종양내침윤림프구에 대한 양적 평가를 위한 방법으로, 현재 많은 종류의 악성종양에서 그 중요성이 대두되고 있는 Immunoscore를 도입하기로 하였다. 이를 위해 종양 중심과 침윤 경계에 발현된 CD3, CD8 양성 림프구의 밀도를 종양세포 내부와 기질에서 각각 컴퓨터 프로그램을 이용하여 분석하였고, 그에 따라

Immunoscore 0에서 Immunoscore 8까지의 값을 산출하였다. 종양관련대식구에 대한 평가를 위해 CD68과 CD163에 대한 면역조직화학검사를 시행하였고, 이 또한 종양 중심과 침윤 경계에 발현된 종양관련대식구의 밀도를 종양세포내부와 기질에서 각각 컴퓨터 프로그램을 이용하여 분석하여, 0에서 4점까지의 스코어를 산출하였다. 더불어 종양 세포와 기질 내 염증 세포에 대하여 PD-L1 단백의 발현을 평가하였고, Immunoscore의 높고 낮음에 의해 PD-L1이 가지는 예후적 영향이 어떻게 달라지는지에 대해 분석하였다.

결과: CD3, CD8 양성 종양내침윤림프구와 CD68, CD163 양성 종양관련대식구의 밀도는 종양세포 내부에 비해 기질에서 의미 있게 높았다. 생존분석에서 Immunoscore가 높을수록 무병생존률이 높은 경향을 보였고, Immunoscore 5를 기준으로, 미만일 경우 낮은 Immunoscore, 이상을 높은 Immunoscore로 정의하여, 다변량 분석을 시행한 결과 높은 Immunoscore의 종양을 가진 환자군의 전체생존률과 무병생존률이 낮은 Immunoscore의 종양을 가진 환자군보다 의미 있게 높았다. 그러나 CD68, CD163 양성 종양관련대식구의 밀도는 예후와 유의한 상관 관계를 보이지 않았다. PD-L1 단백의 발현은 환자의 예후와 별다른 상관 관계를 보이지 않았으나, Immunoscore와 PD-L1 발현을 조합하여, 4개의 군으로 나누어 시행한 생존 분석 결과 PD-L1의 발현이 높은 환자라도 Immunoscore에 따라 생존률이 의미있게 달라짐을 확인할 수 있었다. 즉 다변량 분석에서 PD-L1의 발현이 양성을 보이는 종양을 가진

환자군에서 Immunoscore가 높은 군이 낮은 군보다 전체 생존률이 의미있게 높음을 확인할 수 있었다.

결론: Immunoscore는 현미부수체불안정성 위암에서 의미 있는 예후 인자로 사용될 수 있음을 확인하였다. 또한 Immunoscore와 PD-L1 발현과의 조합을 통해, 종양의 내인성 경로에 의해 PD-L1의 발현이 유도된 환자군이 종양 미세환경 내 적응면역체계에 의해 PD-L1의 발현이 유도된 환자군에 비해 유의하게 나쁜 예후를 보인다는 것을 확인하였다.

주요어: 위암, 현미부수체불안정성, 종양내침윤림프구, 종양관련대식구, 종양 미세환경, PD-L1

학 번: 2012-31139